JCEC
THE JOURNAL OF ENGINEERING AND EXACT SCIENCES

OPEN ACCESS

The Journal of Engineering and Exact Sciences – jCEC, Vol. 09 N. 05 (2023)
journal homepage: https://periodicos.ufv.br/jcec
eISSN: 2527-1075
ISSN: 2446-9416

Parametric study of rider's comfort in a vehicle with semi-active suspension system under transient road conditions

Article Info:
Article history: Received 2021-10-22 / Accepted 2023-01-20 / Available online 2023-01-20
doi: 10.18540/jcecvl9iss5pp15287-01e

Arinola Bola Ajayi
ORCID: https://orcid.org/0000-0002-4733-0803
Department of Mechanical Engineering, University of Lagos, Lagos, Nigeria
E-mail: abajayi@unilag.edu.ng
Ediketin Ojogho
ORCID: https://orcid.org/0000000155662683
Department of Aerospace Engineering, Lagos State University, Ojo, Lagos, Nigeria
E-mail: ediketin96@gmail.com
Surajudeen Adedotun Adewusi
ORCID: https://orcid.org/0000000161455744
Mechanical & Transportation Technology Department, Algonquin College, Ottawa. Canada
E-mail: adewuss@algonquincollege.com
Sunday Joshua Ojolo
ORCID: https://orcid.org/0000-0002-4548-0090
Department of Mechanical Engineering, University of Lagos, Lagos, Nigeria
E-mail: sojolo@unilag.edu.ng
Julio Cesar Costa Campos
ORCID: https://orcid.org/0000-0002-9488-8164
Federal University of Viçosa, Brazil
E-mail: julio.campos@ufv.br
Antonio Marcos de Oliveira Siqueira
ORCID: https://orcid.org/0000-0001-9334-0394
Federal University of Viçosa, Brazil
E-mail: antonio.siqueira@ufv.br

Abstract
Considering that many Nigerian roads are untarred, the effect of frequent plying of these untarred roads on passengers and the expected performance of suspension system of vehicles are important for health and safety reasons. This is significant because the transmission of vibration associated with suspension systems are dependent on the frequency range of the road parameters type the nature of the suspension system and the vehicle seating arrangement that is producing the vibration. Thus, this study focuses on the discomfort experienced by passengers based on parametric study of vehicle with semi-active suspension system under transient road conditions. The modeling of the of semi-active vehicle suspension system properties are contrived on the mass- spring damper system for 4 degree-of–freedom half- car model integrated with 3 degrees of freedom human-seat arrangement. Using vehicle parameters, the severity of ride discomfort experienced by the passenger as the vehicle traversed transient road conditions (i.e., traversing obstruction) was evaluated in terms of the vibration dose value (VDV). Results of simulation based on the parametric studies are presented and the vibration dose values evaluated to show the dependence of vehicle ride comfort on the characteristics of the various elements of the vehicle suspension such as stiffness and damping characteristics. The result showed that the variation of sprung mass and suspension

stiffness of the vehicle had more significant effects on passenger discomfort than the variation of the unsprung mass. The parametric study also revealed that suspension stiffness affects the suspension working space as the vehicle traversed transient road condition.

Keywords: Frequency spectrum. Half-car Model. Ride discomfort. Semi-active suspensions. Transient road condition. Vibration dose value.

Nomenclature

$a_1,\ a_2,\ a_3$ distance between front and rear suspensions and the vehicle body from center of center of gravity

c_2, c_3 Damper of ower and upper limb

$C_{sf}\ , C_{sr}$ Front and rear suspension damper of sprung mass

C_{uf}, C_{ur} Front and rear suspension damper of unsprung mass

F_{df}, F_{dr} Damping forces of the front and rear half-car suspension model

$F_{sf},\ F_{sr}, F_{uf}, F_{ur}$ Upward force on the system due to front suspension and rear suspension of sprung and unsprung masses

$F_{u,}F_z$ Force function of front and rear control and force function of road input

$h_0,$ Height of road bump

G Center of gravity

J Polar Moment of inertia

k_2, k_3 Spring constant of the lower and upper limb

$k_{se},\ c_{se}$ Spring and damper of seat

$K_{sf}\quad K_{sr}$ Front and rear suspension stiffness of sprung mass

$K_{uf}\ ,\ K_{ur}$ Front and rear suspension stiffness of unsprung mass

m_b Vehicle body mass

m_{se}, m_2, m_3 Masses of seat, lower limb and upper limb

M_{Sf}, M_{sr} Sprung masses of front and rear suspensions

M_{uf}, M_{ur} Unsprung masses of front and rear suspensions

$q_b,\ \dot{q}_b$ Vertical displacement and velocity of seat

$u_f\ , u_r$ Control forces of the front and rear suspension

$v_0,$ Velocity of vehicle

w_b Width of road bump

x_b The vertical displacement of sprung mass about the center of gravity

x_{se}, x_2, x_3 Displacements of seat, lower and upper limb

$\dot{x}_{se}, \dot{x}_2, \dot{x}_3$ Velocities of the seat, lower and upper limb

$\ddot{x}_{se}, \ddot{x}_2, \ddot{x}_3$ Accelerations of the seat, lower and upper limb

x_{sf}, x_{sr} Vertical displacement of front and rear sprung mass about the center of gravity

$x_{uf}\ x_{ur},$ Vertical displacement of the front and rear unsprung mass

$z_f(t),\ z_r(t)$ Sinusoidal road induced disturbance to the front and rear wheels

$z, \dot{z}$ Displacement and velocity of the road input function

$z_f,\ z_r$ Disturbances at the front and the rear due to the movement of the vehicle over an uneven road disturbance

$\dot{z}_{f,}\ \dot{z}_r$ Velocities of the front and rear due to road input

ω Circular frequency of road distribution

$\theta,\ \dot{\theta},\ \ddot{\theta}$ Angular displacement Pitch rate of change and Angular acceleration of the body

1. Introduction

Road conditions have tremendous effects on vehicle's Centre of gravity (CG) acceleration, axle acceleration, suspension working space, dynamic tire loading, dampers and spring forces, etc. The influence of the road profile in relation to the comfort and health of passengers is an important consideration because road unevenness causes a form of excitations for a moving vehicle and affects the accelerations of sprung mass and unsprung mass of the suspension system. The varying vehicle speed and road profile impact the frequency spectrum of vehicle oscillation. Thus, when a vehicle moves on rough terrain at variable speeds, it's sprung mass and unsprung mass have different motions which cause dynamic response of the chassis, driving characteristics, vehicle braking characteristics, passengers' comfort and health, and vehicle's safety (Blundel, 1999). Consequently, the effect of some tropical and developing world roads on vehicle suspension system and the attendant consequences on the health of passengers in those vehicles calls for concern and is the motivation for this work. This is significant as it will create the awareness of the influence of the undulating nature of rough roads particularly on suspension system, discomfort experienced by passengers, and the related health issues ranging from passengers back pain to fatigue to mention just a few. The responses of passengers and drivers to road disturbances can be evaluated on the basis of the rider's comfort on a vehicle which is an important parameter (Griffin, 1990). The vibrating frequency response of the rider, the excitation spectrum and the time of exposure play important roles in ride comfort of vehicles.

Many research works had been done in the area of rider's discomfort on a vehicle. For example, Jones and Saunder (1972) exposed 30 men and 30 women participants for 8 second vibrating input in a study experiment in unrestricted sitting positions on a vibrating plate. Griffin (1992) used Laboratory based evaluation method of discomfort produced by vibration. This method made use of shake table rig (motion simulator). The set- up was carried out to produce the feeling of being in a vehicle that is moving. Niekerk et al. (2002) used 16 subject participants in a test, and combinations of six different automotive seats attached to a vibrator. Another approach used to quantify discomfort involves the situation where the vehicle dynamic effects are isolated by defining the comfort in relation to the vibration level of the seat (Mansfield, 2005). This approach was used by many researchers to carry out objective measurement to predict ride comfort with vehicle occupant participating in the measurement. Hacaambwa and Giacomin (2007) measured the subjective response of a human participant in a seating position in a small vehicle driven on a road and the analysis was carried out for 15 seconds in order to quantify ride discomfort experienced by the rider.

Several car models such as quarter-car (Q-car), Segla and Reich (2001), Faheem et al (2006), Jacquelien et al (2006); Half-car (H-car) model by Senthilkumar and Vijayarangan (2007), and Full-car (F-car) by Blundel (1999) and Guglielmino et al. (2008) have been developed to study riders' discomfort. In the quarter-car model, 2 degrees of freedom was considered in its simplest form and it used vertical displacement with a single wheel. The quarter-car model is usually used for suspension analysis because of its simplicity and captures the important parameters of the full car model. In vehicle system dynamics, the quarter-car model has been employed on many occasions to assess the ride performance of vehicles (Sharp and Hassan, 1986; Thompson, 1989).

However, the quarter-car model did not consider pitching, yaw and rolling motions which are important, in particular, during the traversing of obstacles such as bumps and potholes. Thus, alternative models are the half-car models which provide knowledge about the pitch, roll and bounce of the vehicle body and produce quite satisfactory results for transient conditions **(**Ihsan et al., 2007). When a vehicle traversed irregular road profile, the road excitation characteristics influence its ride performance and handling stability (Gohrle et al. 2014; Kim and Choi 2016). As a result, suspension plays a critical role in the transmission of force between vehicle tire and body and reduces the effect of the road surface on the vehicle occupants (Kim and Choi 2016). Although most passenger vehicles provide acceptable ride comfort on smooth road surfaces, some performed poorly when travelling on rough terrain such as potholes and bumps (Sharp and Hassan 1986). As

a result, shocks are generated which are reduced to a considerable extent by tires, springs and shock absorbers.

Many researchers had investigated the response of the half-car model in relation to the road conditions. Lin and Kortum (2007) carried out a time-domain direct identification of parameters for vehicle mass, damping and stiffness while Akcay and Turkay (2009) studied multi-objective control of half-car suspension system. They noticed that proper estimation of the tire damping coefficients led to road holding quality of the suspension system, vehicle handling, braking for good safety and drive pleasure, keeping the occupants of the vehicle comfortable and secluded from road noise, bumps and vibration. They used frequency domain method to estimate the suspension system parameters and frequency response of half-car model, due to pavement roughness, accessed the ride quality and comfort. Deriving data through experimental method, it was observed that the damping coefficients of the tire can be estimated and the road holding quality of the suspension system parameters can be improved by using frequency domain method (Akcay and Turkay, 2009).

Using the application of linear switched reluctance motor as active suspension system in half car model, the ride's comfort best performance and handling quality under all driving conditions was achieved by considering the vehicle body as an elastic assembly **(**Zhang et al 2010) while Fischer and Isermann (2004) determined ride comfort using the relationship between the parameters of the half-car model and road roughness defined by acceleration value of the response of the suspension system.

Using half-car model parameters (Soliman et. al 2013) carried out design and modeling, through simulation to determine the relationship between road roughness and passenger comfort, while Miliken (1995) investigated kinematic response measures such as bump and roll camber angles which are design requirements for the suspension components of vehicle. The nonlinearity of the road profile due to the unevenness and smoothness of the road surface and control performance for half car suspension system of mass, damping and stiffness indicates that the behavior of the vehicle under different excitations (road conditions) - bumps or potholes is used to reveal the transient characteristics of the road disturbance (Akcay and Turkay, 2009). In the transient state, the vehicle travels with varying vehicle velocities, while in steady state, constant vehicle velocity were performed using direct identification for vehicle mass, damping and stiffness, **(**Gao and Zing, 2010 and Thite et al, 2011).

Methods for assessing the transient response of a vehicle include computer simulation (Sharp and Hassan, 1986) or theoretical analysis by mathematical modeling (Thompson, 1989) or experimental testing either on the road or on the ride simulator in the laboratory (Olatunbosun and Dunn, 1991). Computer aided analysis is fast becoming an important tool in the development of suspension system. One of such tools are based on Matlab/Simulink software which has been adopted and implemented by several researchers to analyze the response of vehicles traversing road irregularities (Olatunbosun and Dunn, 1991).

Dynamic simulation of automotive suspension system has become significant for improving vehicle ride comfort and safety (Zhaoling, 2002). The use of computer aided analysis has the ability to determine the effects of parameter changes early in the design process and to reduce development cost (Simon and Ahmadian, 2001). In general, investigations of vehicle dynamic analysis require reduction of the vehicle system to a mathematical model which becomes the representation of the vehicle (Sharp and Hassan, 1986 and Thompson, 1989).

Automotive suspension system also employs asymmetric dampers which exhibit high damping coefficient in the rebound than in compression. It was pointed out that the reason for such asymmetry was not quantified explicitly (Dixon, 2007). However, it is most likely due to high dependence of vehicle performance on the damping asymmetry properties (Anderson and Fan, 1990). Also, the effect of damping asymmetry is highly influenced by the type of excitation and suspension responses. Researchers have investigated the suspension properties and their effects on various vehicle performance extensively (Duym et al, 1997 and Basso, 1998). Only some few researchers have attempted to quantify the effects of asymmetric damping on vehicle counteractions to transient excitations using bumps and potholes (Verros et al., 2000; Simms and Crolla, 2007).

Road profile simulations are also carried out using power spectral density, PSD which generate road profile signals. Many procedures had been presented in literature for the generation of random time signal with given spectral density using periodic functions (Rouillard et al. 2008 and Sun, 2002). The governing mathematical model of the dynamics of a system is applied, especially in multi-body systems where the equations of motion can be obtained from numeric algorithms (Haug, 1989) or symbolic algorithms (Bruulseman and McPhee, 2002, and He and McPhee 2007). The values chosen for the system parameters used in the mathematical model, such as spring stiffness, damping coefficient and mass properties, is important in determining the extent to which the model will respond. The collected experimental data from a physical system can be used to determine the model parameters that are difficult to measure directly and to obtain more accurate estimate for parameters that are known approximately (Haug, 2002; Bruulseman and McPhee, 2002).

This study is undertaken in order to assess the discomfort experienced by vehicle occupant and the working space of the suspension of the vehicle using the parameters of the vehicle suspension characteristics and the human biomechanical parameters. A half-car semi-active suspension system combined with a human-seat arrangement was modeled. A transient road condition was considered as input to the suspension system, in which the vehicle was excited by a half sine bump on an otherwise smooth road.

2. Methodology

2.1 Model Description

In this study, a 4 degree of freedom half-car model that has wheels fixed at the two ends of a rigid beam was considered. The end of the car body is allowed to oscillate about its own conjugate point so that the spherical joint for the rear axle is placed in the front of the conjugate point. In this way, the entire mass of the car body is considered in the half-car model which is useful for the accuracy of the results (Shahriar et al, 2016). The wheel and the road generate the forces while the wheels are control elements, having significance in the dynamic behavior of vehicles (Sharp and Hassan, 1986). The spring-damper characteristics are modeled as simple linear system (Hacaambwa and Giacomin, 2007; Jones and Saunder, 1972). The springs and dampers are modeled together as semi-active elements, translational in nature and they are positioned between the car body and the axle (Mohan et al., 2010).

A seat-human subsystem is included in the semi-active vehicle suspension system in order to assess the performance of the model in relation to the ride comfort of the passengers (Mansfield, 2005). By adding a 3 degree of freedom human-seat arrangement to the half-car model, a 7 degree of freedom system is created as shown in the Figure 1. The joints of the human body were represented using spring-damper elements to connect each of the body part (Abbas et al, 2010).

The spring-damper parts in the human body are translational. The body interacts with the suspension through the seat. The seat is modeled by mass m_{se} spring stiffness k_{se} and damper c_{se} while the human sub-system is composed of lower and upper body masses m_2 and m_3; the spring stiffness and damping properties of the lower and upper bodies segments are k_2 and k_3 , damper c_2 and c_3 respectively. The point C represents the driver or passenger position and point B, located at a distance a_3 from the center of gravity of the vehicle body is the distance between the vehicle body and the seat–driver subsystem.

Semi-active suspension is a type of automotive suspension systems that controls the damping force of the shock absorber in response to input from the continuously varying road surfaces. It is intended to approximately implement the active suspension with a damping force adjustable shock absorber. The performance of the semi-active system implies that the sprung mass acceleration, suspension deflection and tire deflection are all significantly improved at the first natural frequency.

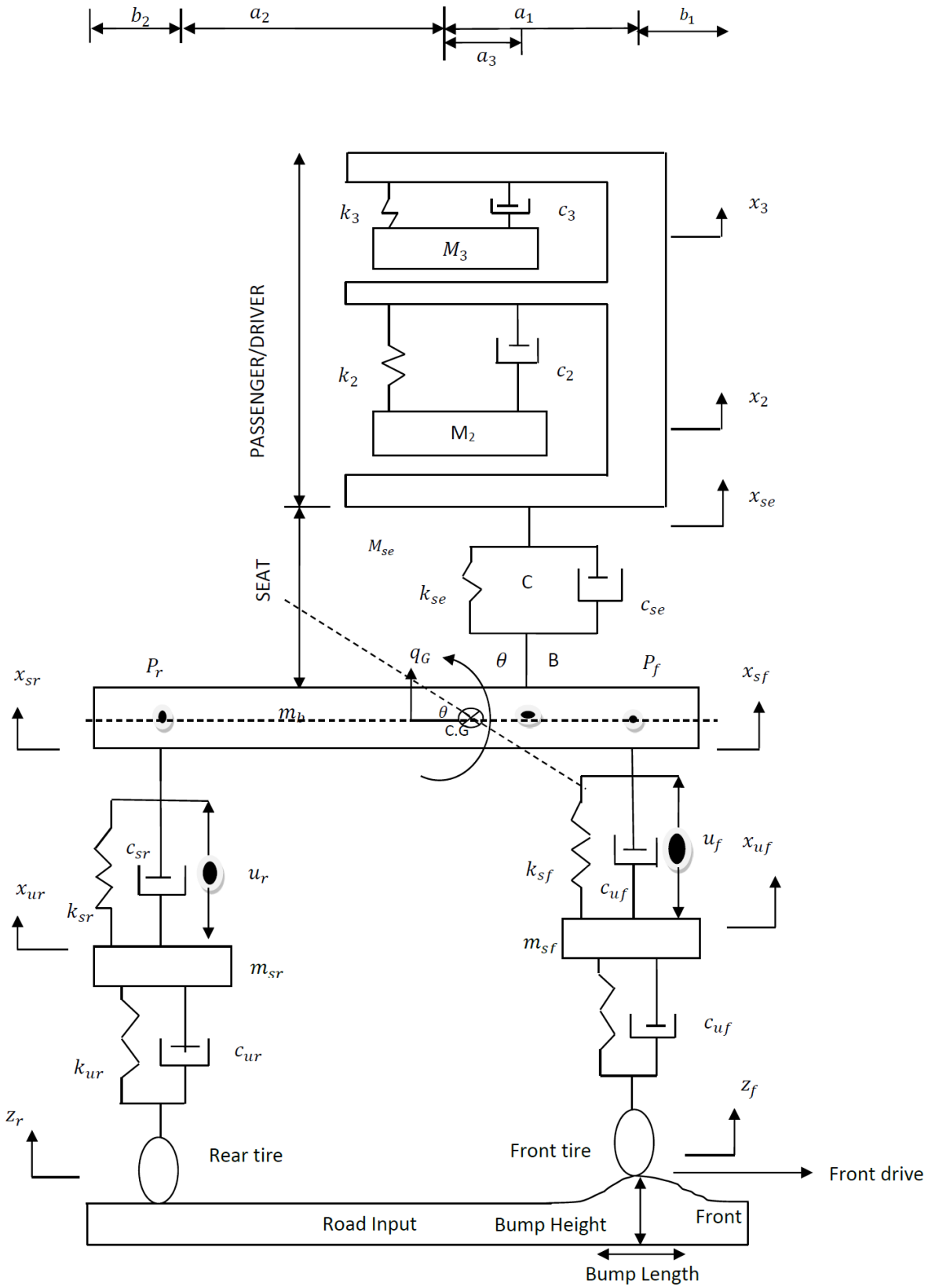

Figure 1: Half-car vehicle model with human-seat

2.2 Mathematical Modeling

A 7 degree of freedom (d.o.f) model consisting of 4 d.o.f half-car semi-active suspension combined with 3 d.o.f human-seat biodynamic model is adopted order to model and investigate the rider's discomfort on a passenger vehicle with semi-active suspension system, traversing transient road condition. The semi-active half-car suspension system incorporates magneto rheological, (MR) dampers which offers the advantages of passive and active suspension systems. MR dampers usage in vehicles suspension is attributed to their ease, high dynamic range, low power requirement, large force capacity and robustness (Wei and Lin, 2007).

The half-car model is used because it takes into account both translational bounce motion about any axis) and rotational motions (pitch motion about the y axis) of the sprung mass. This assumes the car is symmetric about the longitudinal axis and also assumes equal suspension characteristics for both front wheels and rear wheels (Olatunbosun and Dunn, 1991). This is shown in Figure 2. In this study, the half-car model was adopted because it captured the important characteristics of the full car model in simulating pitch, and heave or bounce motions, and the pattern followed by the displacements and acceleration of the sprung mass was the same as that of the full car model. However, in this study, the roll motion of the half-car is not considered.

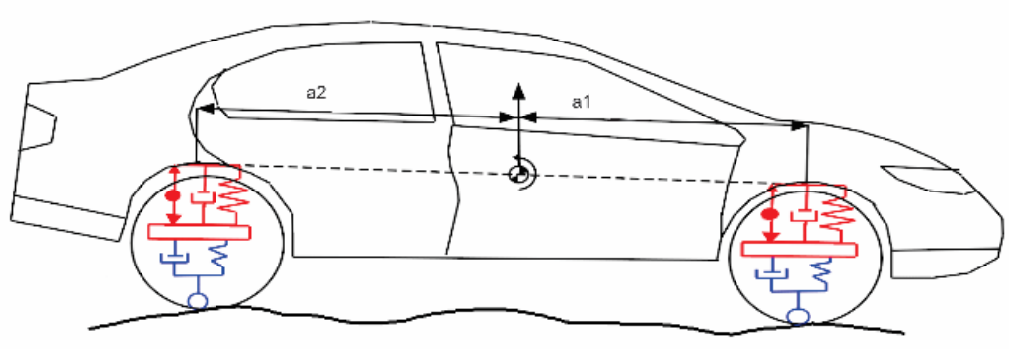

Figure 2: Schematic diagram of a half-car model

Half car models are classified into roll degree of freedom and pitch degree of freedom models, each model having 4-degrees of freedom. In the roll degree of freedom model, the vehicle is considered to be half at the rolling axis. In other words, when the disturbance or shock at the left wheel of the front axle is isolated, then the effect at the right wheel of front axle is also considered. In the pitch degree of freedom, pitching axis is the point of separation. The pitch model of the half-car is considered in this study. It is the rotation angle about the lateral axis which allows the analysis of road excitation to be applied to both wheels of the vehicle. Pitch motion occurs as an outcome of the difference between the upward movement of the front and rear suspensions of the vehicle. The model for this study is considered on the basis of vehicle wheel base, suspension stiffness and damping characteristics and height of road unevenness.

In the half-car model, specific values such as vehicle body mass, the vehicle body mass moment of inertia, masses of the front and rear wheels, distance of the front or rear suspension location to the center of gravity of the vehicle body, stiffness of front and rear tires, damping coefficients and spring stiffness of front and rear suspensions are considered. However, the model presents the following assumptions: The contact with the road is a point contact. This is a simple model of the tire, springs and dampers which are considered linear, with single point attachments of the springs which restrict the degree of freedom in the axles and frame and only the vertical displacement of suspension is considered.

2.2.1 Vehicle coordinate system: The coordinate system of a vehicle showing the roll, pitch and yaw in the x, y and z directions is shown in Figure 3, according to Dorsch (2014).

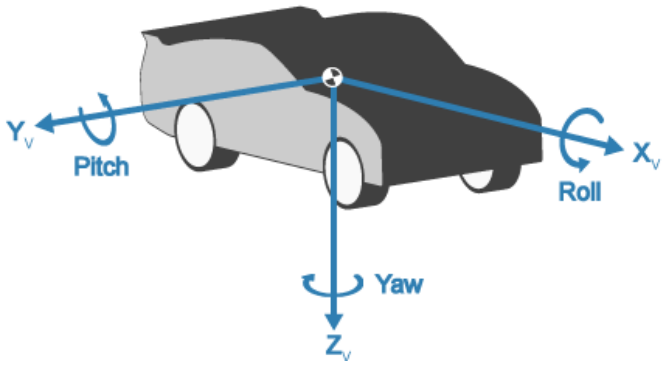

Figure 3: Vehicle coordinate system

The vehicle fixed coordinate system which has its origin fixed at the center of gravity of the vehicle and travels with vehicle was used in order to define a relative coordinate system for the dynamics of the suspension components when studying the suspension system (Chace, 1967). According to ISO 2631 (1997), the positive directions of the axes are defined as follows: (i) X-Axis is straight to the front from vehicle. (ii) Y-Axis is straight to the right from the vehicle. (iii) Z-Axis points downward from the vehicle.

The motion of the vehicle is described in terms of six degrees of freedom relative to the origin of the coordinate system of the vehicle which includes three translational and three rotational degrees of freedoms about the principal axes. These motions include the following: (i) Longitudinal motion: the body motion in the x-axis dimension or forward/backward. For example, as the vehicle accelerates or brakes, its body is excited with forces in this direction (longitudinal force). (ii) Lateral motion: the body motion in the y-axis dimension or left/right. The centrifugal lateral force exerted on the vehicle during turning is an example. (iii) Vertical motion: the body motion in the z-axis dimension or up/down. An example is an upward and downward motion of the vehicle body caused by uneven road profile. This is the heave or bounce motion usually measured at the mass center of the vehicle body. It is an important parameter in the performance of vehicle suspension. (iv) Roll motion is the rotation of body motion about the x-axis. An example for the excitation of roll motion is when a vehicle is negotiating a corner. The performance of vehicle suspension system provides roll stability for the vehicle. (v) Pitch motion is the rotation of the body motion about the y-axis. The dive of the vehicle body during braking is an example of the pitch body motion. (vi) Yaw motion is the rotation of the vehicle body motion about the z-axis. The spinning motion of a vehicle is an example.

2.2.2 The mathematical model: The mathematical model of the road profile was derived as follows: the vehicle wheel base, w_b passing over each bump with speed V km/h will have front vertical displacement, z_f . The rear wheel followed the same track as the front at a given time delay, τ. In this study, it was assumed that the vehicle model travelled with constant velocity of 20 km/h, bump length 0.5 m and bump height 0.05 m. However, the model adopted in this study did not consider the yaw and roll motions as only the half-car pitch degree of motion is adopted.

The seven degrees of freedom resulting from half-car and human-seat suspension model are governed by equation (1) – (7) as shown as follows:

$$m_3\ddot{x}_3 + c_3(\dot{x}_3 - \dot{x}_{se}) + k_3(x_3 - x_{se}) = 0 \quad (1)$$

$$m_2\ddot{x}_2 + c_2(\dot{x}_2 - \dot{x}_{se}) + k_2(x_2 - x_{se}) = 0 \quad (2)$$

$$m_{se}\ddot{x}_{se} + c_{se}\dot{x}_{se} + c_2(\dot{x}_{se} - \dot{x}_2) + c_3(\dot{x}_{se} - \dot{x}_3) + k_{se}x_{se} + k_2(x_{se} - x_2) + k_3(x_{se} - x_3) = c_{se}\dot{q}_b + k_{se}q_b \quad (3)$$

$$m_b\ddot{x}_b + c_{sf}(\dot{x}_{xf} - \dot{x}_{uf}) + c_{sr}(\dot{x}_{sr} - \dot{x}_{ur}) + k_{sf}(x_{sf} - x_{uf}) + k_{sr}(x_{sr} - x_{ur}) + c_{se}\dot{q}_b - k_{se}q_b + c_{se}\dot{x}_{se} + k_{se}x_{se} = u_f + u_r \quad (4)$$

$$m_{uf}\ddot{x}_{uf} + c_{uf}\dot{x}_{uf} + c_{sf}(\dot{x}_{uf} - \dot{x}_{sf}) + k_{uf}x_{uf} + k_{sf}(x_{uf} - x_{sf}) = -u_f + c_{uf}\dot{z}_f + k_{uf}z_f \quad (5)$$

$$m_{ur}\ddot{x}_{ur} + c_{ur}\dot{x}_{ur} + c_{sr}(\dot{x}_{ur} - \dot{x}_{sr}) + k_{ur}x_{ur} + k_{sr}(x_{ur} - x_{sr})v = -u_r + c_{ur}\dot{z}_r + k_{ur}z_r \quad (6)$$

$$J\ddot{\theta} + a_1c_{sf}(\dot{x}_{sf} - \dot{x}_{uf}) - a_2c_{sr}(\dot{x}_{sr} - \dot{x}_{ur}) + a_1k_{sf}(x_{sf} - x_{uf}) - a_2k_{sr}(x_{sr} - x_{ur}) + a_3c_{se}\dot{q}_b + a_3k_{se}q_b - a_3k_{se}x_{se} - a_3c_{se}\dot{x}_{se} = a_1u_f - a_2u_r \quad (7)$$

If the seat undergoes small rotation at a distance a_3 about the center of gravity, the vertical displacement of the seat is approximated as equation (8a):

$$q_b = x_b - a_3\theta \quad (8a)$$

Differentiating equation (8a) twice, we have equation (8b) and (8c) respectively:

$$\dot{q}_b = \dot{x}_b - a_3\dot{\theta} \quad (8b)$$

$$\ddot{q}_b = \ddot{x}_b - a_3\ddot{\theta} \quad (8c)$$

If the vehicle body undergoes small rotation about the center of gravity CG, equations (9a) and (10a) approximations hold for the vertical displacement of the front sprung mass and the vertical displacement of the rear sprung mass. Carrying out two successive differentiations of the equations (9a) and (10a), we have (9b), (9c), (10b) and (10c) respectively

$$x_{sf} = x_b - a_1\theta \quad (9a)$$

$$\dot{x}_{sf} = \dot{x}_b - a_1\dot{\theta} \quad (9b)$$

$$\ddot{x}_{sf} = \ddot{x}_b - a_1\ddot{\theta} \quad (9c)$$

$$x_{sr} = x_b + a_2\theta \quad (10a)$$

$$\dot{x}_{sr} = \dot{x}_b + a_2\dot{\theta} \quad (10b)$$

$$\ddot{x}_{sr} = \ddot{x}_b + a_2\ddot{\theta} \quad (10c)$$

Substituting equations (8a) and (8b) into equation (3), and simplify, we have equation (11)

$$m_{se}\ddot{x}_{se} + (c_{se} + c_2 + c_3)\dot{x}_{se} + c_{se}a_3\dot{\theta} - c_{se}\dot{x}_b - c_2\dot{x}_2 - c_3\dot{x}_3 + (k_{se} + k_2 + k_3)x_{se} - k_{se}x_b + k_{se}a_3\theta - k_2x_2 - k_3x_3 = 0 \quad (11)$$

Substituting equations 9 (a) and (b) and equations 10 (a) and (b) into equation (4), we have equation (12)

$$m_b\ddot{x}_b + (c_{sf} + c_{sr} + c_{se})\dot{x}_b + (a_2c_{sr} - a_1c_{sf} - a_3c_{se})\dot{\theta} + (a_2k_{sr} - a_1k_{sf} - a_3k_{se}) + (k_{sf} + k_{sr} + k_{se})x_b - c_{sf}\dot{x}_{uf} - c_{sr}\dot{x}_{ur} - k_{sf}x_{uf} - k_{sr}x_{ur} - c_{se}\dot{x}_{se} - k_{se}x_{se} = u_f + u_r \quad (12)$$

Substituting equations (9a) and (9b) into equation (5), we obtain equation (13)

$$m_{uf}\ddot{x}_{uf} - c_{sf}\dot{x}_b + c_{sf}a_1\dot{\theta} + (c_{uf} + c_{sf})\dot{x}_{uf} + (k_{uf} + k_{sf})x_{uf} - k_{sf}x_b + k_{sf}a_1\theta = -u_f + c_{uf}\dot{z}_f + k_{uf}z_f \quad (13)$$

Substituting equations (10a) and (10b) into equation (6), and simplify, we obtain equation (14)

$$m_{ur}\ddot{x}_{ur} - c_{sr}\dot{x}_b - a_2c_{sr}\dot{\theta} + (c_{ur} + c_{sr})\dot{x}_{ur} - k_{sr}x_b + (k_{sr} + k_{ur})x_{ur} + a_2k_{sr}\theta$$

$$= -u_r + c_{ur}\dot{z}_r + k_{ur}z_r \quad (14)$$

Substituting equations (8a), (8b), (9a), (9b), (10a) and (10b) in equation (7), and simplify we have equation (15)

$$\begin{aligned} J\ddot{\theta} + \left(a_1c_{sf} - a_2c_{sr} + a_3c_{se}\right)\dot{x}_b - \left(a_2{}^2c_{sr} + a_1{}^2c_{sf} + a_3{}^2c_{se}\right)\dot{\theta} - a_1c_{sf}\dot{x}_{uf} + a_2c_{sr}\dot{x}_{ur} \\ + a_1k_{sf}x_{uf} - a_2k_{sr}x_{ur} + \left(a_1k_{sf} - a_2k_{sr} + a_3k_{se}\right)x_b \\ - \left(a_1{}^2k_{sf} + a_2{}^2k_{sr} + a_3{}^2k_{se}\right)\theta - a_3k_{se}x_{se} - a_3c_{se}\dot{x}_{se} = a_2u_r - a_1u_f \quad (15) \end{aligned}$$

Expressing equations (1), (2), (11), (12), (13), (14) and (15) in matrix form, we have equation (16), the generalized system equation of motion as

$$[M]\{\ddot{x}\} + [C]\{\dot{x}\} + [K]\{x\} = \{F\} \quad (16)$$

Where

$$[M] = \begin{bmatrix} m_3 & 0 & 0 & 0 & 0 & 0 & 0 \\ 0 & m_2 & 0 & 0 & 0 & 0 & 0 \\ 0 & 0 & m_{se} & 0 & 0 & 0 & 0 \\ 0 & 0 & 0 & m_b & 0 & 0 & 0 \\ 0 & 0 & 0 & 0 & m_{uf} & 0 & 0 \\ 0 & 0 & 0 & 0 & 0 & m_{ur} & 0 \\ 0 & 0 & 0 & 0 & 0 & 0 & J \end{bmatrix}$$

$$[C] = \begin{bmatrix} c_3 & 0 & -c_{se} & 0 & 0 & 0 & 0 \\ 0 & c_2 & -c_{se} & 0 & 0 & 0 & 0 \\ -c_3 & -c_2 & c_{se}+c_2+c_3 & -c_{se} & 0 & 0 & c_{se}a_3 \\ 0 & 0 & C_{se} & c_{sf}+c_{sr}+c_{se} & -c_{sf} & -c_{sr} & c_{sr}a_2 - c_{sf}a_1 - c_{se}a_3 \\ 0 & 0 & 0 & -c_{sf} & c_{uf}+c_{sf} & 0 & c_{sf}a_1 \\ 0 & 0 & 0 & -c_{sr} & 0 & c_{ur}+c_{sr} & -c_{sr}a_2 \\ 0 & 0 & c_{se}a_3 & c_{sf}a_1 - c_{sr}a_2 + c_{se}a_3 & -c_{sf}a_1 & c_{sr}a_2 & -\left(c_{sr}a_2{}^2 + c_{sf}a_1{}^2 + c_{se}a_3{}^2\right) \end{bmatrix}$$

$$[K] = \begin{bmatrix} k_3 & 0 & -k_3 & 0 & 0 & 0 & 0 \\ 0 & k_2 & -k_2 & 0 & 0 & 0 & 0 \\ -k_3 & -k_2 & k_{se}+k_2+k_3 & k_{se} & 0 & 0 & k_{se}a_3 \\ 0 & 0 & -k_{se} & k_{sf}+k_{sr}+k_{se} & -k_{sf} & -k_{ur} & k_{sr}a_2 - k_{sf}a_1 - k_{se}a_3 \\ 0 & 0 & 0 & -k_{sf} & k_{uf}+k_{sf} & 0 & k_{sf}a_1 \\ 0 & 0 & 0 & -k_{sr} & 0 & k_{sr}+k_{ur} & k_{sr}a_2 \\ 0 & 0 & k_{se}a_3 & k_{sr}a_2 - k_{sf}a_1 + k_{se}a_3 & k_{sf}a_1 & -k_{sr}a_2 & k_{sf}a_1{}^2 + k_{sr}a_2{}^2 + k_{se}a_3{}^2 \end{bmatrix}$$

$$[F_u] = \begin{Bmatrix} 0 \\ 0 \\ 0 \\ u_f + u_r \\ -u_f \\ -u_r \\ a_1u_f - a_2u_r \end{Bmatrix} \text{ and } [\boldsymbol{F_z}] = \begin{Bmatrix} 0 \\ 0 \\ 0 \\ 0 \\ k_{uf}z_f + c_{uf}\dot{z}_f \\ k_{ur}z_r + c_{ur}\dot{z}_r \\ 0 \end{Bmatrix} = \begin{Bmatrix} 0 \\ 0 \\ 0 \\ 0 \\ \left(k_{uf} + j\omega c_{uf}\right)z_f \\ \left(k_{ur} + j\omega c_{ur}\right)z_r \\ 0 \end{Bmatrix}$$

$\dot{z}_f = j\omega z_f, \quad \dot{z}_r = j\omega z_r$ are time derivative of z_f *and* z_r respectively

$[M]$, $[C]$ and $[K]$ are mass, damping and stiffness matrices respectively;
$\{X\}$, $\{\dot{x}\}$ and $\{\ddot{x}\}$ are the displacement, velocity and acceleration vectors respectively;
$[F_u]$ and $[\mathrm{F_z}]$ are the force functions.

The vectors $\{z_f\}, \{\dot{z}_f\}, \{z_r\}, \{\dot{z}_r\}$ are displacements and velocities of front and rear tires due to road input.

Based on the passenger vehicle model for the study, displacement vector, velocity vector and acceleration vector matrices are formulated as shown equation (17).

$$\{x\} = \begin{Bmatrix} x_3 \\ x_2 \\ x_{se} \\ x_b \\ x_{uf} \\ x_{ur} \\ \theta \end{Bmatrix} \{\dot{x}\} = \begin{Bmatrix} \dot{x}_3 \\ \dot{x}_2 \\ \dot{x}_{se} \\ \dot{x}_b \\ \dot{x}_{uf} \\ \dot{x}_{ur} \\ \dot{\theta} \end{Bmatrix} \{\ddot{x}\} = \begin{Bmatrix} \ddot{x}_3 \\ \ddot{x}_2 \\ \ddot{x}_{se} \\ \ddot{x}_b \\ \ddot{x}_{uf} \\ \ddot{x}_{ur} \\ \ddot{\theta} \end{Bmatrix} \quad (17)$$

For example, displacements of the upper body, x_3 of passenger comes before that of the lower body, x_2 etc. The quantities are also in accordance with the equations (1), (2), (11), (12), (13), (14) and (15).

2.3 Input Road Profile Excitation

The sinusoidal road profile excitation is adopted to analyze the proposed model to be able to assess the transient performance of the suspension system. The sinusoidal road induced disturbance for the front and rear wheels are assumed as in equations (18) and (19) (Alireza and Salim, 2006; Shirahatt, et. al 2008; and Gao and Zing, 2010).

$$z_f(t) = h_0 sin(\omega t_1) \quad (18)$$
$$z_r(t) = h_0 sin(\omega t_2) \quad (19)$$

Where $t_2 = t_1 + \tau$
t_1 is the time required for the front wheel to impact the bump,
t_2 is the time required for the rear wheel to impact the bump, and
τ is the delay time for the rear wheel to impact the bump.

The sinusoidal induced disturbance for the front wheel is given in equation (20) (Stutz and Rochinha, 2011) as:

$$z_f(t) = \begin{cases} h_0 sin\left(\frac{\pi v_0 (t-t_0)}{w_b}\right) & \forall \quad t_0 \le t \le t_0 + \frac{w_b}{v_0} \\ 0 & \forall \quad t \le t_0 \; or \; t > t_0 + \frac{w_b}{v_0} \end{cases} \quad (20)$$

Where $\omega = \frac{\pi v_0}{w_b}$ is the circular frequency of road disturbance,
h_0 = the height of the road irregularities (bump)
w_b = width of the road irregularities (bump) which has sinusoidal profile with half wavelength and
t_0 = initial time of the impact;
v_0 = velocity of the vehicle.

2.4 Suspension Parameters and Simulation of Semi-active Half-car Suspension System with Human Seat Arrangement

Appropriate parameter selection in vehicle suspension system analysis is aimed at providing an isolation of vehicle body from road irregularities and to ensure passengers' comfort. The first aim involves ride analysis and how discomfort experienced by riders of the vehicle can be reduced.

The second aim is in the area of road holding analysis. The design goal of vehicle suspension system is to minimize both the acceleration of the vehicle body and the suspension working space for a given vehicle suspension value.

The parameters utilized in this study were obtained from a mid-sized saloon (Raji, 2013) car. This is significant because of the widespread use of this type of vehicle for passengers, its lower cost of purchase, effects of vibration on the vehicle occupants and the ride performance characteristics of the vehicles as they traversed different road conditions. These parameters are given in Table 1.

Table 1: Suspension parameters (Raji, 2013)

Parameter	Symbol	Values	Unit
Sprung mass of vehicle chassis	m_b	575	kg
Moment of inertia of the vehicle	J	769	kgm^2
Unsprung mass of the front axle	m_{uf}	60	kg
Unsprung mass of the rear axle	m_{ur}	60	kg
Stiffness of the front tire	k_{uf}	190	kN/m
Stiffness of the rear tire	k_{ur}	190	kN/m
Damping coefficient of front tire	c_{uf}	350	Ns/m
Damping coefficient of rear tire	c_{ur}	350	Ns/m
Stiffness of the front suspension	k_{sf}	16812	N/m
Stiffness of the rear suspension	k_{sr}	16812	N/m
Damping coefficient of the front suspension	c_{sf}	1000	Ns/m
Damping coefficient of the rear suspension	c_{sr}	1000	Ns/m
Front body length from CG	a_1	1.35	m
Rear body length from CG	a_2	1.45	m
Seat-driver distance from CG	a_3	0.65	m

Table 2: Human Biomechanical parameters (Abbas et al, 2010)

Parameter	Symbol	Values	Unit
Mass of lower limb	m_2	5.5	kg
Mass of upper limb	m_3	36	kg
Stiffness of lower limb	k_2	144000	N/m
Stiffness of upper limb	k_3	20000	N/m
Damping coefficient of lower limb	c_2	909	Ns/m
Damping coefficient of upper limb	c_3	330	Ns/m

2.5 Simulink Block Diagram for Road Bump

Simulink block diagram as shown in Fig. 4 is developed to investigate the dynamic response of the vehicle model under transient road conditions. Using the vehicle system model equations (1, 2, 11, 12, 13, 14 and 15); equations (16) in matrices form and the transient road conditions equations (18 and 19), computer simulations are carried out. In the transient condition, the vehicle traverses a half sine obstacle with dimension of 0.05 m maximum height and 0.5 m long. The vehicle model parameters and the biomechanical model parameters of human system used for the computer simulations were given in Tables 1 and 2.

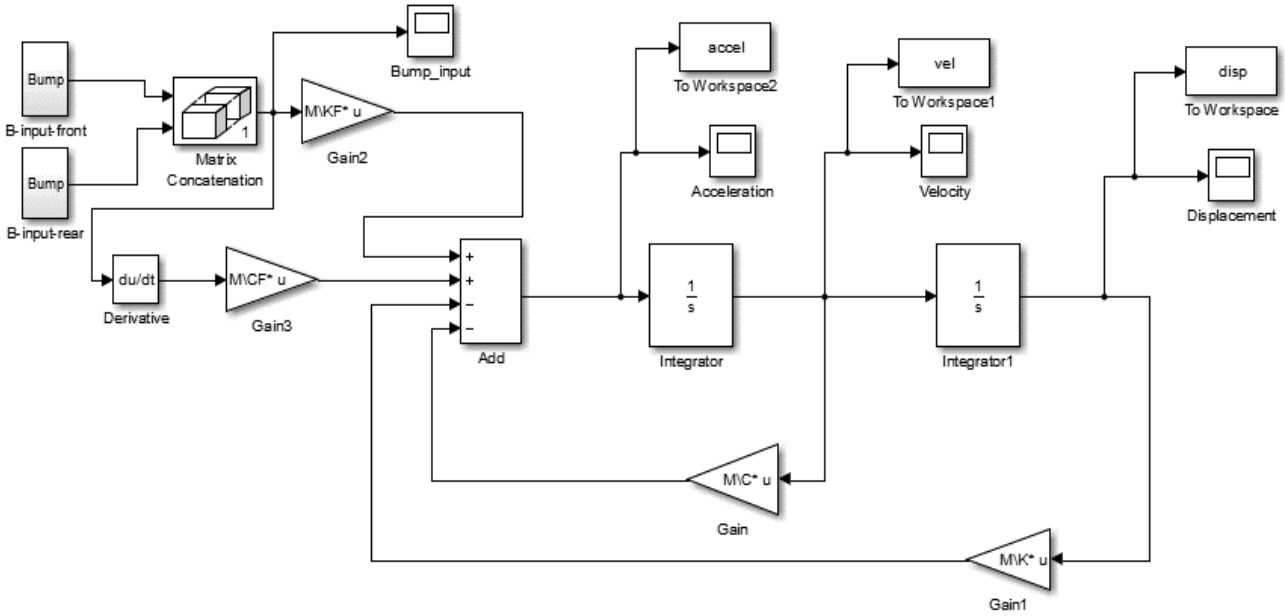

Figure 4: Simulink block diagram for road bump under transient road conditions

3. Results and Discussions

Responses of vehicle suspension system to transient road condition using the parameters in Tables 1 and 2 and the Simulink block diagram are shown in Figures 5 – 10. The simulations are based on the mathematical model for a 4 degree of freedom half-car model combined with a 3 degree of freedom human subsystem-seat model. The car is assumed to be moving at a speed of 20km/h at the time it traversed the half-sine bump of height 0.05 m and length 0.5 m.

3.1 Responses of Vehicle Suspension System to Transient Condition

For the given input parameters, the performance of the vehicle was observed on basis of the responses of the vehicle suspension system via simulation using Matlab/Simulink block diagram which was developed using the model equations of motion. The simulation results are shown in Figures 5 – 10. The observed parameters of the model were suspension displacements and accelerations of the lower and upper body of the passenger, displacement of vehicle chassis, pitch angle of the vehicle body, displacement of front and rear wheel, acceleration of passenger seat and chassis.

Figure 5 shows the response of the upper and lower parts of the human body. The upper body produced a higher displacement compared to the lower body. Both upper and lower bodies responded to a settling time longer than 3.5 seconds (the time required by the system response to reach specified range of it final value for the first time). This is due to the shift in the center of gravity of the vehicle because of the inclusion of the human seat arrangement in the vehicle model. It may also be due to the vibration received by the upper body from the seat combined with that induced by the lower body.

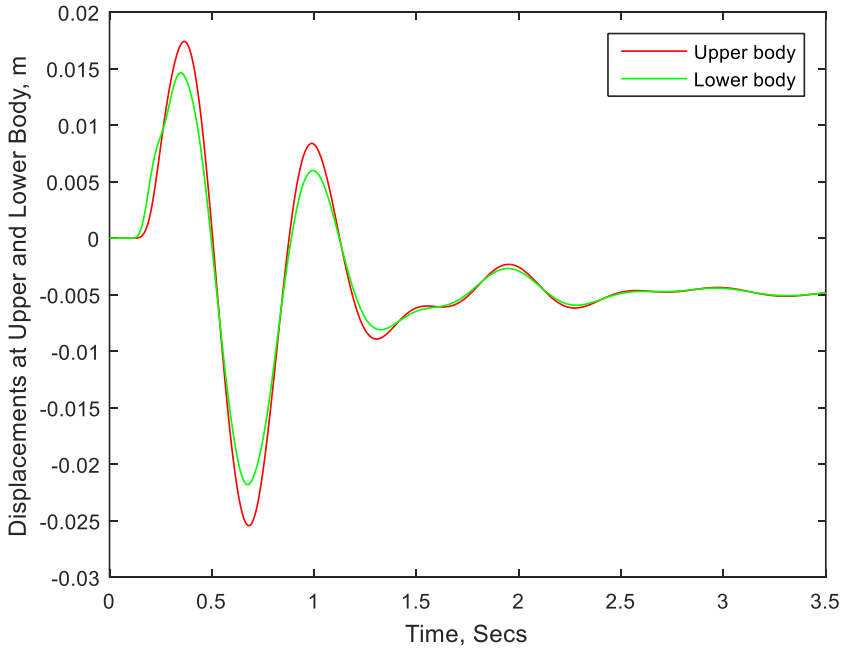

Figure 5: Displacement of upper and lower body of the rider in a vehicle passing over a bump obstacle, 0.05 m height and 0.5 m length

Figure 6 shows the acceleration responses of the upper and lower body of the human subsystem. The upper body has a higher vertical acceleration compared to the lower body. This is due to the higher displacement experienced by the upper body as the vehicle traversed the bump. Thus, it took the upper body longer settling time compared to the lower body. This is due to the period of time over which vibration occurred in the upper body. But both took settling time longer than 3.5 seconds.

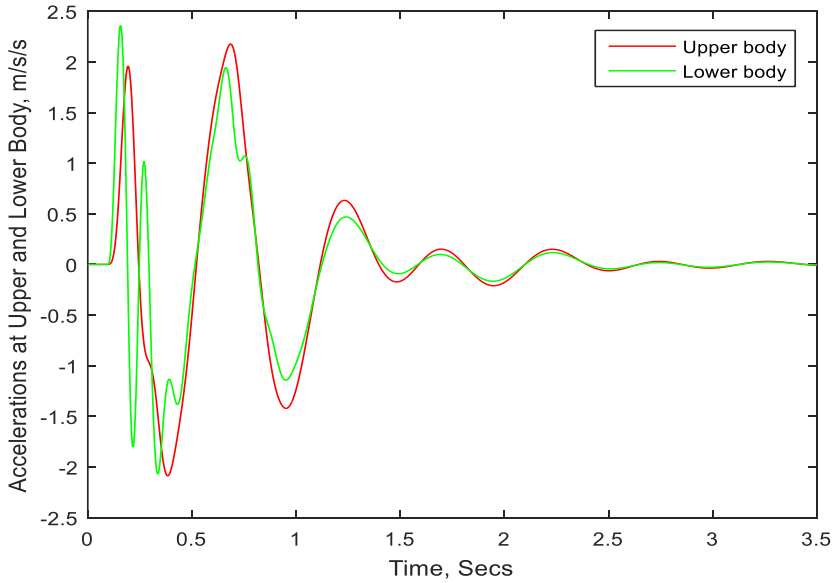

Figure 6: Acceleration of upper and lower body for vehicle passing over a bump obstacle, 0.05 m height and 0.5 m length

Figure 7 depicts the responses of the front and rear chassis vertical displacements. Both took longer settling time, although the settling time of the rear chassis was longer than 3.5 seconds compared to the front chassis with settling time of about 3.0 seconds. This is perhaps due to the time delay (the required by the system response to reach half of its final value for the first time) between the front and rear chassis when the vehicle traversed the bump. This is because the rear wheel traversed the bump later than the front wheel.

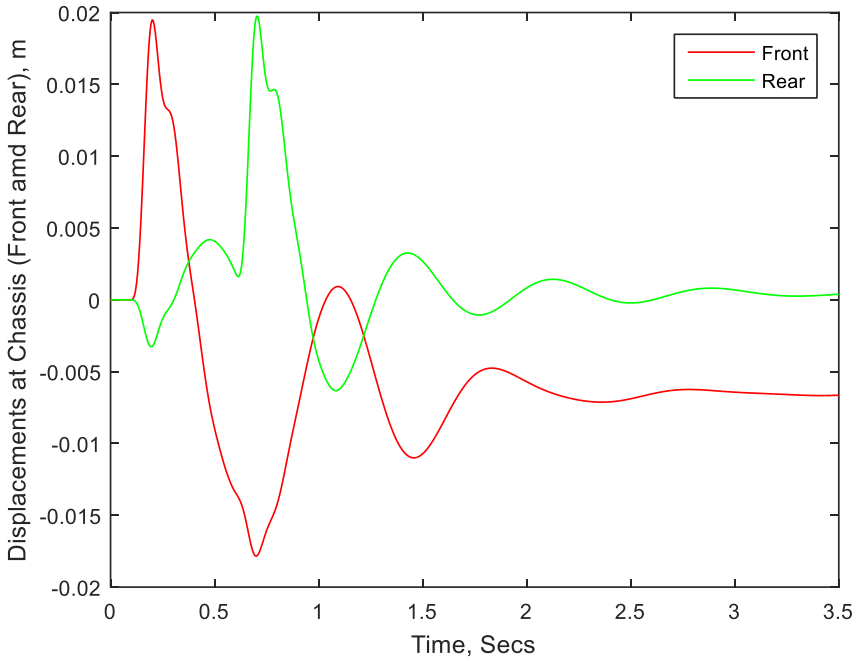

Figure 7: Displacement at chassis for vehicle passing over a bump obstacle, 0.05 m height and 0.5 m length

Figure 8 shows the pitch response of the vehicle. Again, it took a settling time of almost 3.5 seconds.

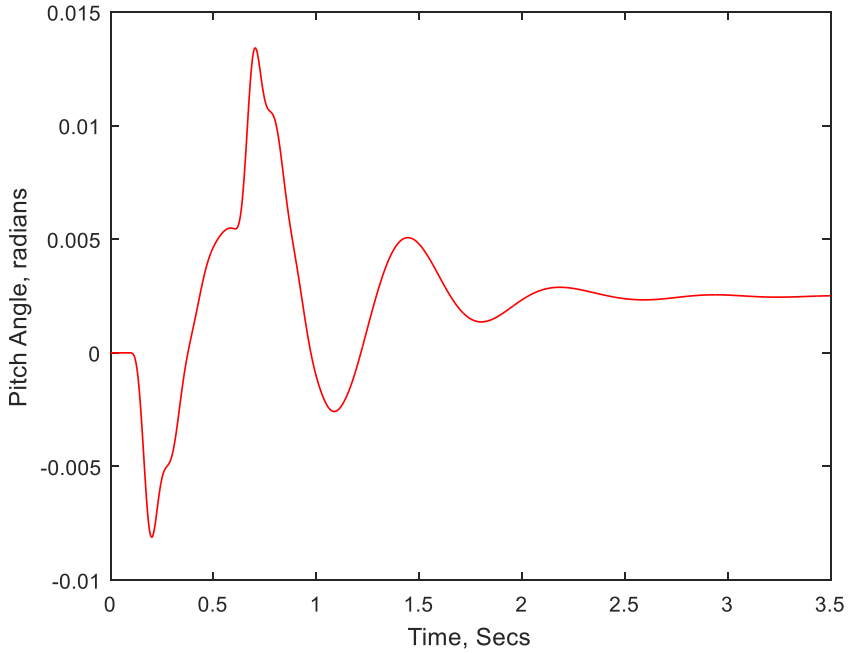

Figure 8: Pitch Angle for vehicle passing over a bump obstacle, 0.05 m height and 0.5 m length

Figure 9 shows the responses of the front and rear wheel as the vehicle traversed the bump. The settling time of the front wheel was about 1.7 seconds compared to the rear wheel with a settling time of about 1.2seconds. This is because the front wheel traversed the bump earlier before the rear wheel. The response shows that when the front wheel goes over bump, rear wheel stayed on ground which causes reduction in the displacement and acceleration of the vehicle body. When the rear wheel reaches the bump, the front wheel was on the ground which also causes a reduction in displacement. Thus, Figure 9 showed that the settling time of the rear wheel was faster compared to the front wheel.

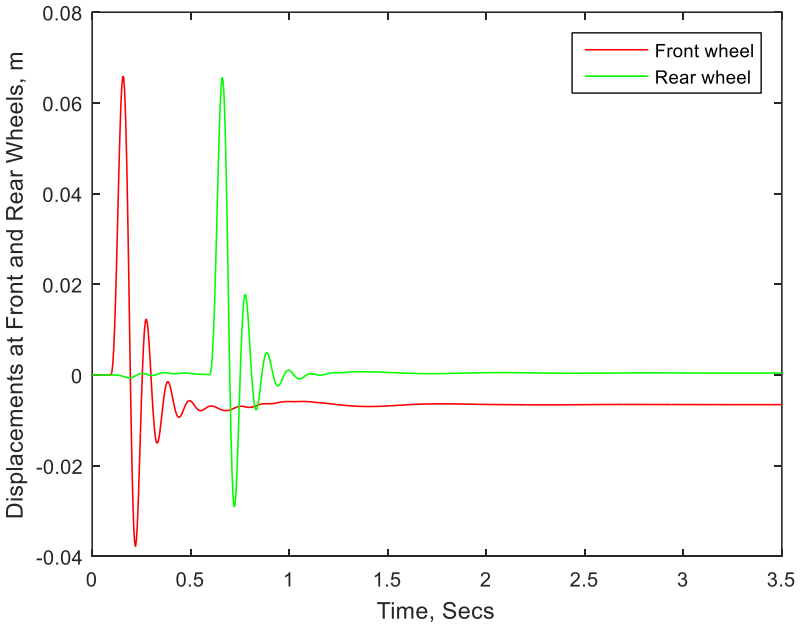

Figure 9: Displacement at Front and Rear Wheels for vehicle passing over a bump obstacle, 0.05 m height and 0.5 m length

Figure 10 shows the acceleration responses of the seat and chassis about the center of gravity, C.G.

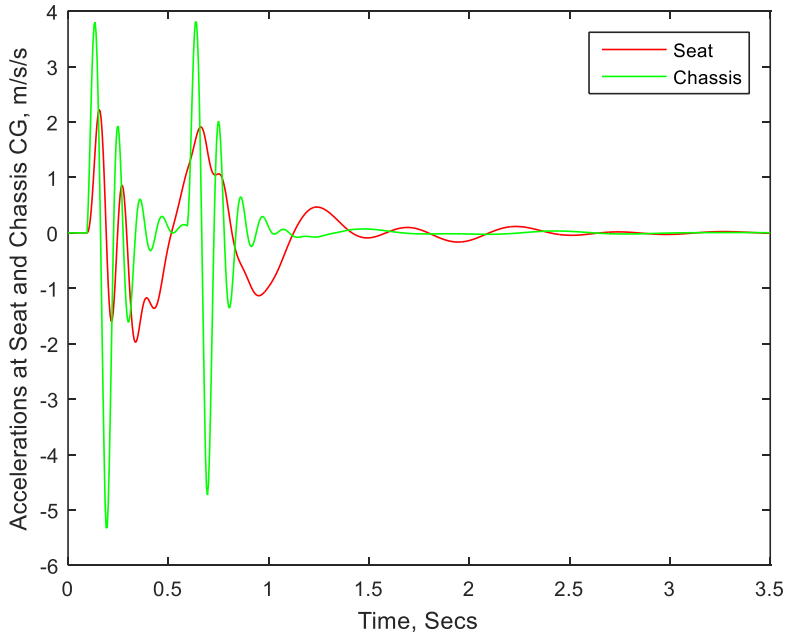

Figure 10: Acceleration at Seat and Chassis C.G for vehicle passing over a bump obstacle, 0.05 m height and 0.5 m length

The seat has a higher acceleration at the center of gravity compared to the chassis. This is perhaps due to the shift in the center of gravity of the vehicle because of the inclusion of human seat arrangement with the half-car vehicle model. Also, the settling time of the chassis of about 1.7 seconds was faster than the settling time of the seat of about 3.5 seconds.

3.2 Vehicle Discomfort Parameters

For transient ride, the ride performance is assessed in terms of the vibration dose value, (VDV) which is a cumulative measure of the vibration transmitted to the body of passengers as the vehicle traverses the obstruction. It is calculated by the fourth root of the integral with respect to the time of the fourth power of the acceleration. The use of the fourth power (Paddan and Griffin, 2002) makes the VDV more sensitive to peaks in the acceleration waveform. The vibration dose value, VDV gives a measure of the total exposure of the body to vibration, taking account of the magnitude, frequency and exposure duration. For analysis method based on acceleration, VDV gives the highest correlation between vibration magnitude and discomfort (Paddan and Griffin, 2002). Thus, the VDV $ms^{-1.75}$ defined by BS 6841 (1987), ISO 2631(1997) and Goncalves and Ambrosio (2003), as:

$$VDV = \left(\int_0^T a(t)^4 dt\right)^{\frac{1}{4}} \tag{21}$$

$a(t)$ and T are the acceleration and the period of time over which vibration occur (ISO 2631, 1997 and BS 6841, 1987). According to the BS 6841 (1987), vibration magnitudes and directions that produce VDV in the region of $15\,ms^{-1.75}$ will normally cause severe discomfort. Vibration dose value, VDV measures in $m/s^{1.75}$ shows the total amount of vibration received by human over a period of time. When the motion of a vehicle included shock or impulsive velocity change, the vibration dose value, VDV is considered more suitable for the evaluation of vehicle ride performance. For example, driving on a rough road surface induces high peak and impulses. Thus, the VDV becomes a significant tool for human comfort evaluation.

3.2. Parametric Study of Transient Road Condition

Parameter study was carried out to investigate the effects of various suspension parameters on the passengers' discomfort in transient situation while the vehicle is traversing a half sine road obstacle. The speeds of vehicle traversing the transient road condition were 20 km/h, 30 km/h, 40 km/h, 50 km/h and 60 km/h. Each system parameter: - damping coefficient, tire stiffness, sprung mass and unsprung mass were varied from 80% of the original to 120 % in turn while the other parameters were left unchanged.

Figures 11 – 22 below show the variations of the calculated discomfort of the human system when the damping coefficient, tire stiffness, spring stiffness, sprung mass and unsprung mass were varied. From the responses of the vehicle suspension system for transient road condition, the discomfort experienced by the human body (vibration dose values, VDV) were calculated using equation (21). Figures 11 and 12 show the variation of sprung mass with discomfort at the upper and lower bodies of the passenger respectively. The results showed that the discomfort at the upper bodies (Figure 11) and lower bodies (Figure 12) decreased considerably with increase in sprung mass of the vehicle at a particular vehicle speed but increase as the speed of the vehicle increased from 20 km/h to 60 km/h.

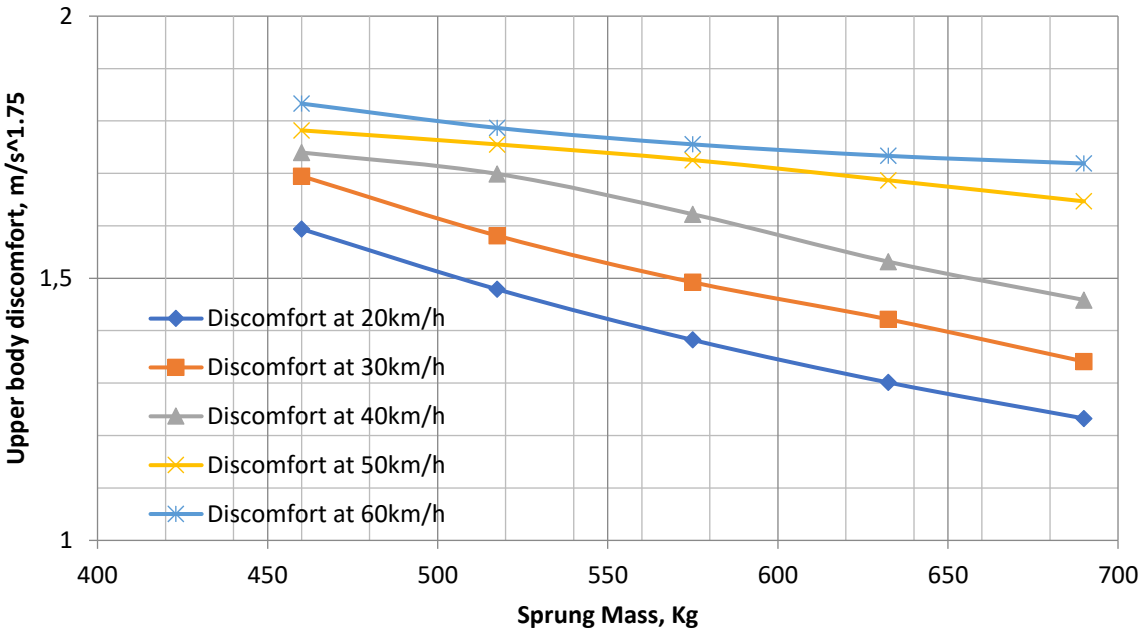

Figure 11: Discomfort at the upper body vs Sprung mass (unsprung mass, suspension damping, suspension stiffness, tire stiffness and tire damping were constant)

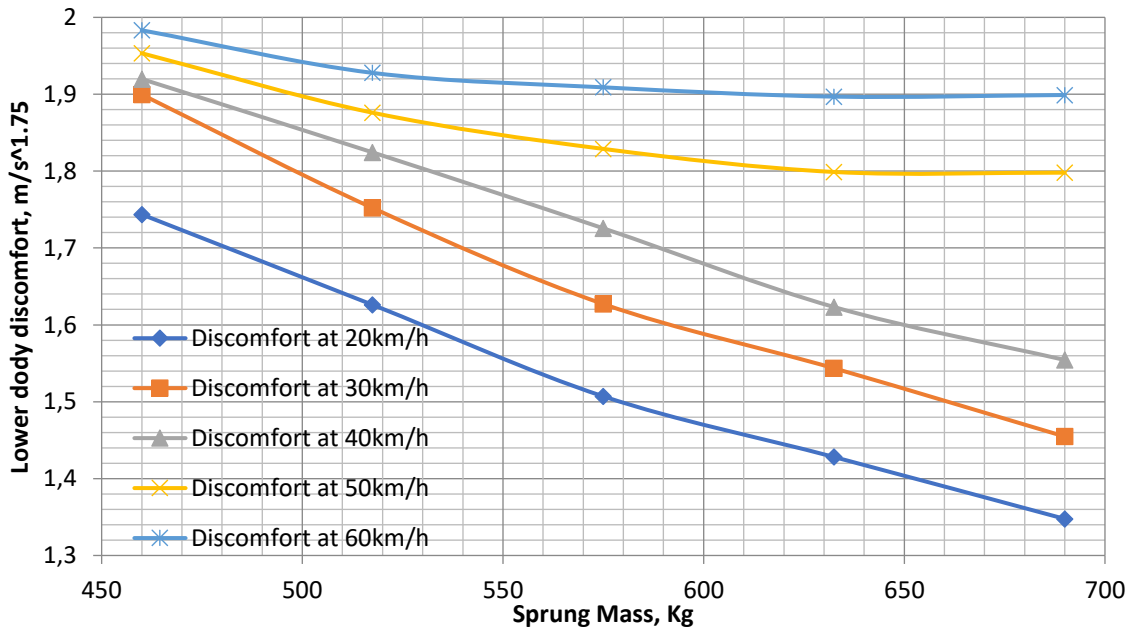

Figure 12: Discomfort at Lower body vs Sprung mass (Unsprung mass, suspension damping, suspension stiffness, tire stiffness and tire damping were constant)

Figures 13 and 14 also showed the variation of unsprung mass in relation to the discomfort at the upper body (Figure 13) and lower body (Figure 14) of the human body as the vehicle traversed irregular road profile. The result indicated that increase in the unsprung mass of the vehicle has little effect on the discomfort of the vehicle occupant but increase with speed of the vehicle.

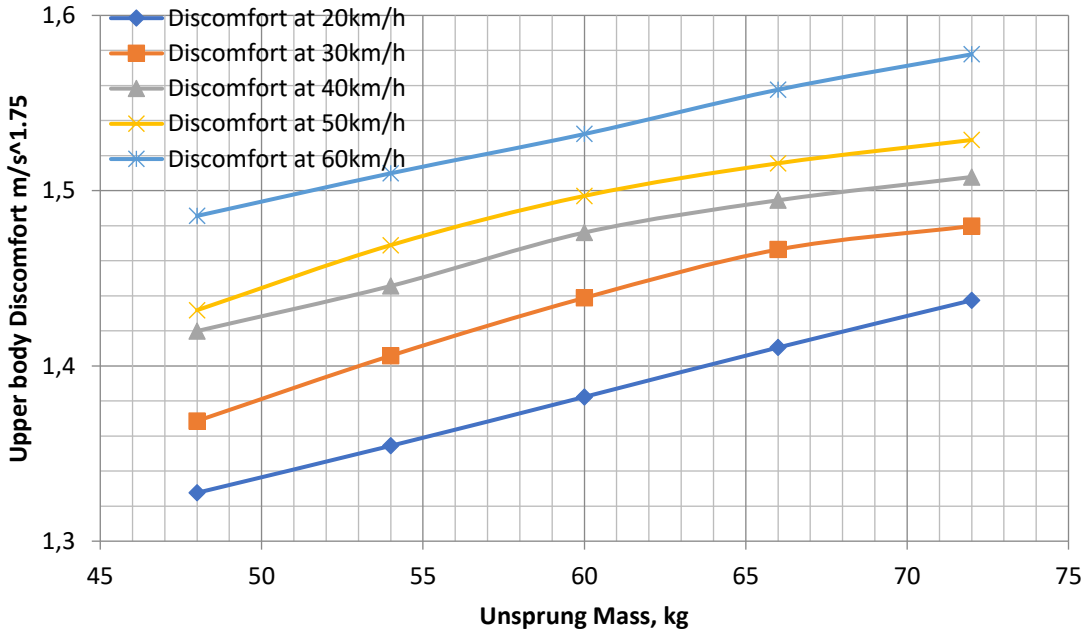

Figure 13: Discomfort at Upper body vs Unprung mass (sprung mass, suspension damping, suspension stiffness, tire stiffness and tire damping were constant)

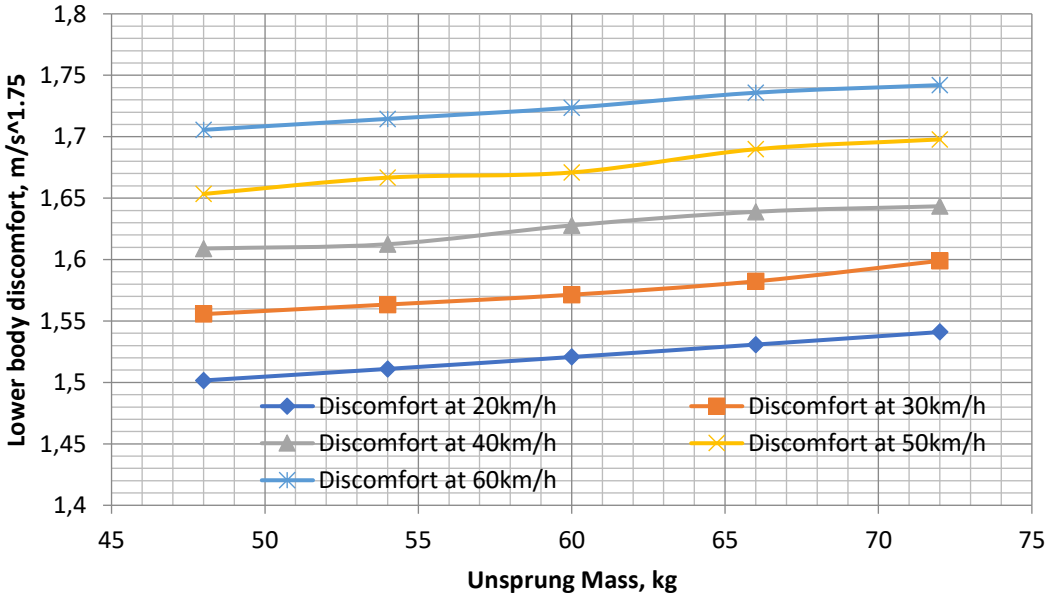

Figure 14: Discomfort at Lower body vs Unprung mass (sprung mass, suspension damping, suspension stiffness, tire stiffness and tire damping constant)

Thus, the variation of the sprung mass has a more significant effect on passenger discomfort than variation of the unsprung mass. These results correlate with that obtained by Blundel (1999) on modeling and simulation of vehicle handling, Senthilkumar and Vijayarangan (2007) on analytical and experimental studies on active suspension system of light passenger vehicle to improve comfort, Olatunbosun and Dunn (1991) in simulation model for passive suspension ride

performance optimization; and Paddan and Griffin (2002) on the effect of seating on exposure to whole-body vibration.

Figures 15 and 16 show the variation of suspension stiffness in relation to the discomfort at the upper body (Figure 15) and lower body (Figure 16) of the vehicle rider. The lower and upper bodies of the rider showed considerable increase in discomfort with increase in suspension stiffness and increase in vehicle speed. The result indicated that increase in the value of the suspension stiffness or vehicle speed had an influence on the lower and upper bodies of the passenger as vehicle traversed road obstacle. The result agreed with that obtained by (Blundel, 1999; Olatunbosun and Dunn, 1991).

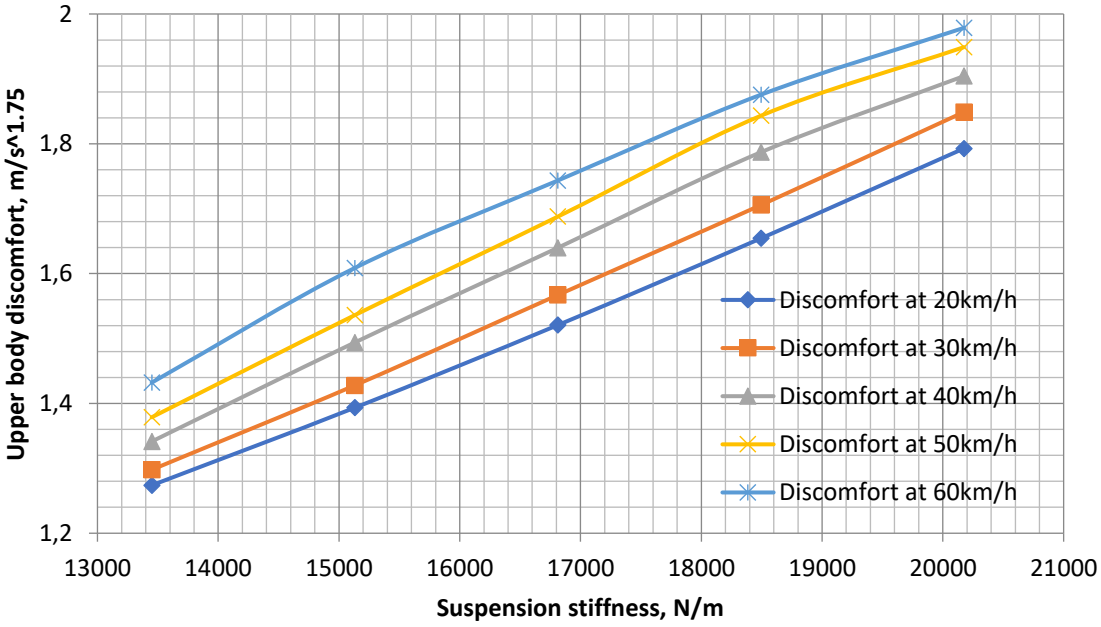

Figure 15: Discomfort at Upper vs Suspension Stiffness (sprung mass, unsprung mass, suspension damping, tire stiffness and tire damping constant)

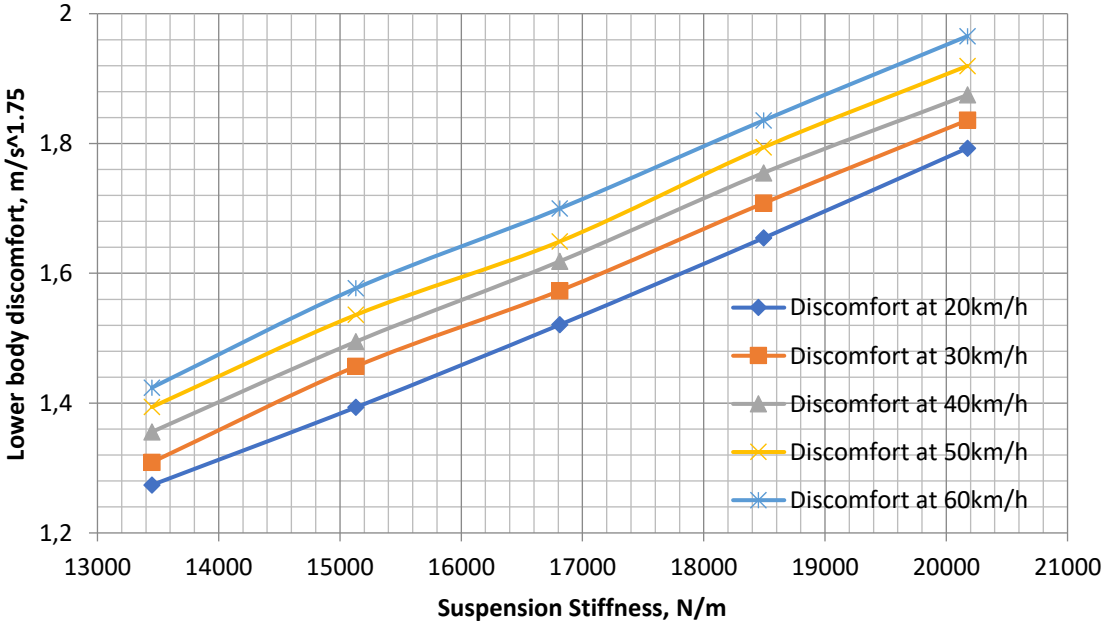

Figure 16: Discomfort at Lower vs Suspension Stiffness (sprung mass, unsprung mass, suspension damping, tire stiffness and tire damping were constant)

Figures 17 and 18 show the relationship between the tire stiffness in relation to the discomfort at the upper and lower bodies respectively. The upper and lower bodies of passenger are sensitive to tire stiffness, the body discomfort increasing rapidly as the tire stiffness and the vehicle speed increased. These results correlate with the results obtained by Sharp and Hassan (1986) on the evaluation of passive automotive suspension system (Olatunbosun and Dunn, 1991 and Paddan and Griffin, 2002).

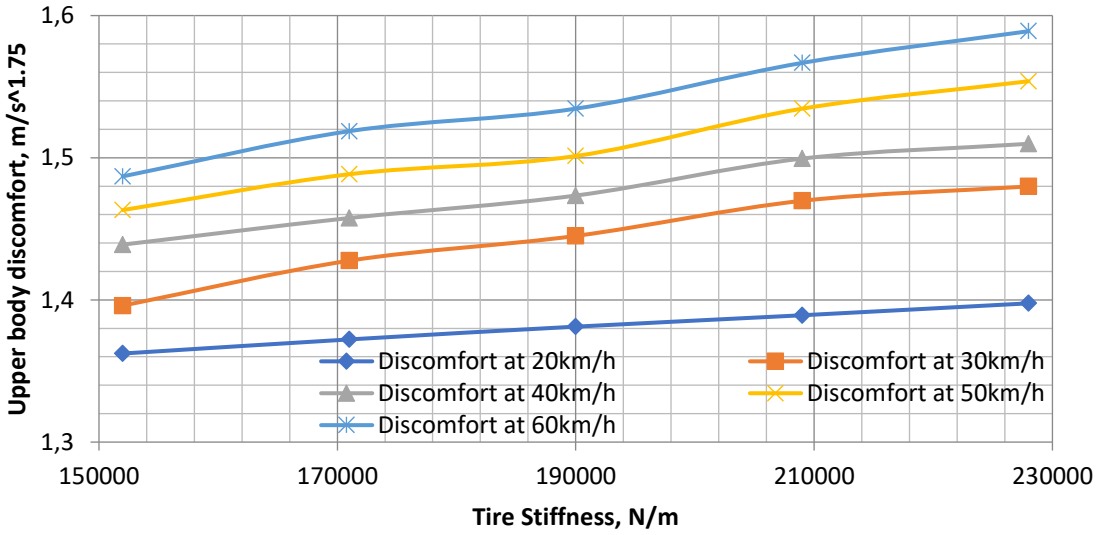

Figure 17: Discomfort at Upper vs Tire Stiffness (sprung mass, unsprung mass, suspension damping, suspension stiffness and tire damping were constant)

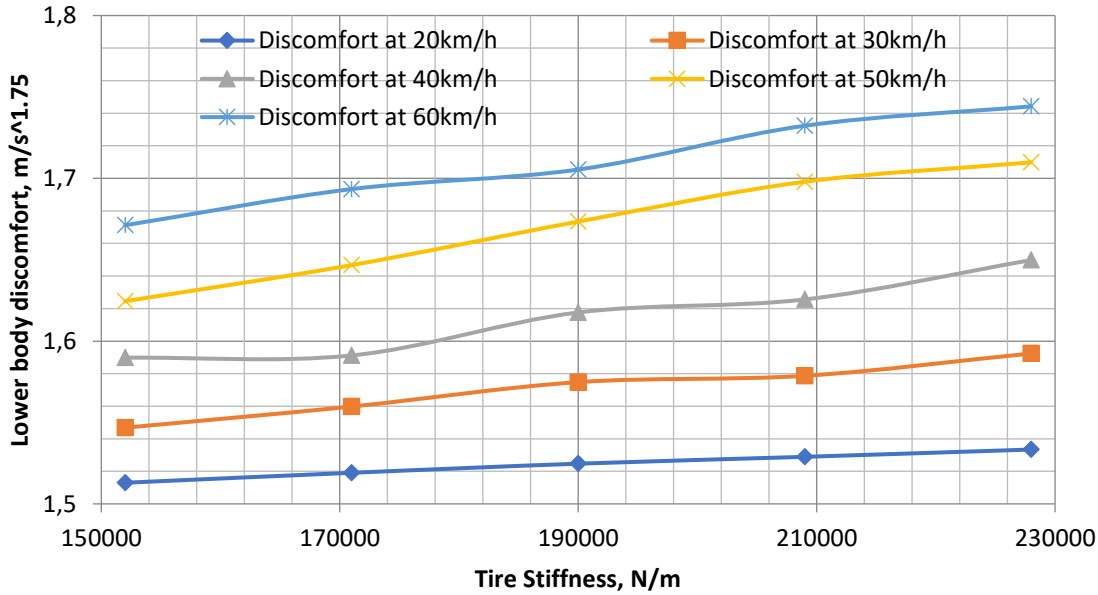

Figure 18: Discomfort at Lower vs Tire Stiffness (sprung mass, unsprung mass, suspension damping, suspension stiffness and tire damping were constant)

The relationship between the tire damping and the rider discomfort at the lower and upper body are shown in Figure 19 and Figure 20 respectively. In Figures 19 and 20, there were little discomfort of the vehicle occupant at the lower and upper bodies due to tire damping. This is due

to the role played by the damper as absorber of vehicle shock when it traversed an obstacle. This agreed with the result obtained by Duym et al (1997), Basso (1998), and Simm and Crolla (2007).

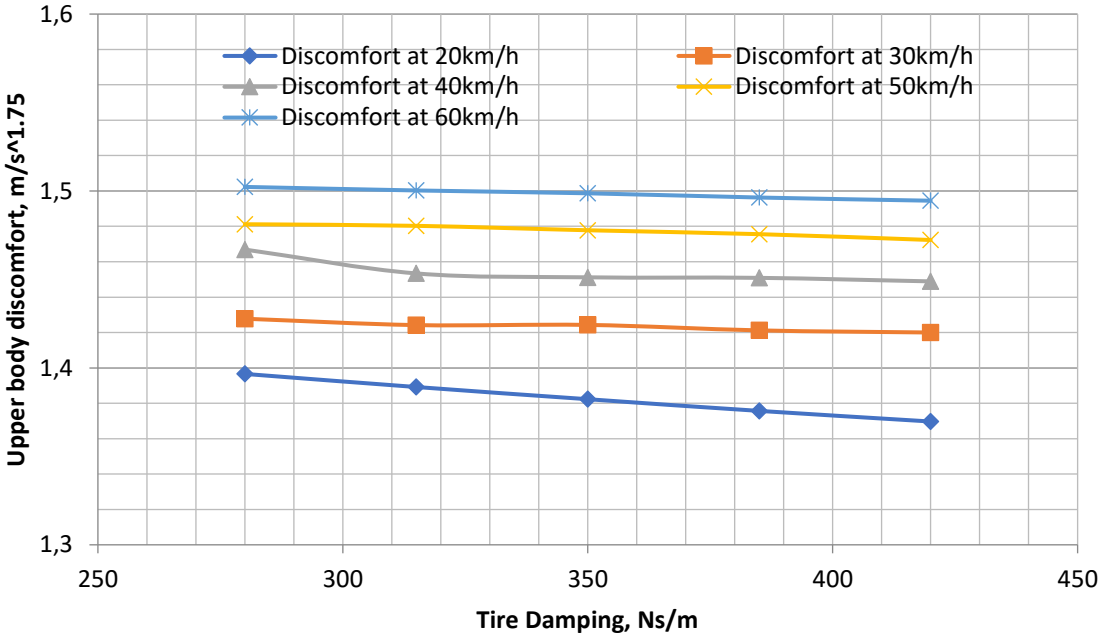

Figure 19: Discomfort at Upper body vs Tire Damping (sprung mass, unsprung mass, suspension damping, suspension stiffness and tire stiffness were constant)

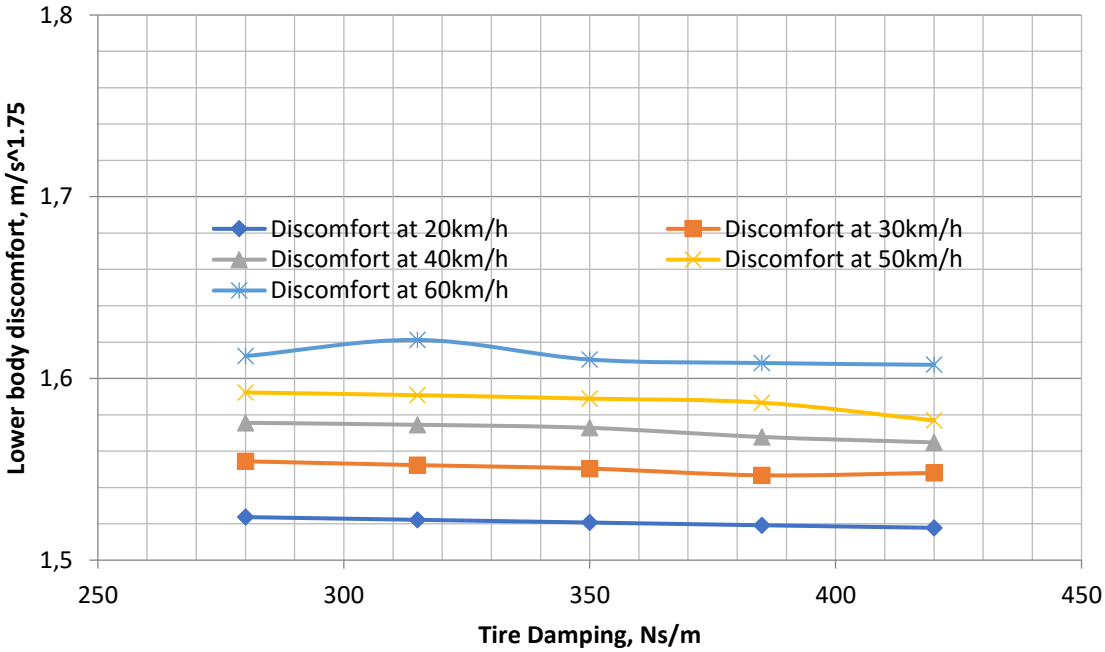

Figure 20: Discomfort at Lower body vs Tire Damping (sprung mass, unsprung mass, suspension damping, suspension stiffness and tire stiffness were constant)

Figures 21 and 22 showed the level of discomfort at the upper and lower bodies of the passenger with increasing suspension damping. The parameter study showed that there was a little variation in discomfort at the upper and lower bodies of the rider while increasing the suspension damping of the vehicle traversing over bump road. The result agreed with that obtained by Sharp and Hassan (1986), Olatunbosun and Dunn (1991), Duym et al (1997), Basso (1998), Simm and Crolla (2007).

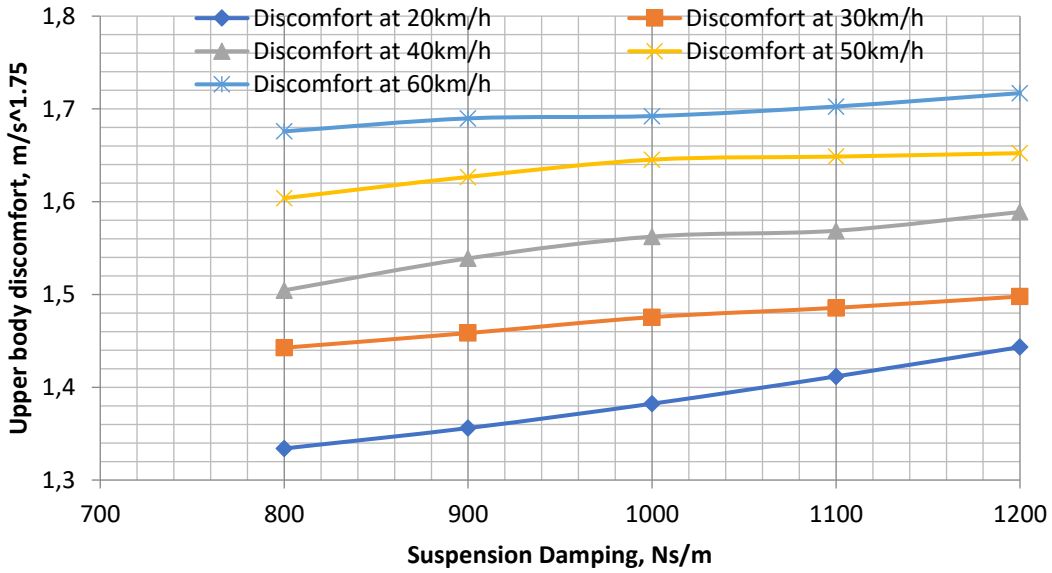

Figure 21: Discomfort at Upper body vs Suspension Damping (sprung mass, unsprung mass, suspension stiffness, tire damping and tire stiffness were constant)

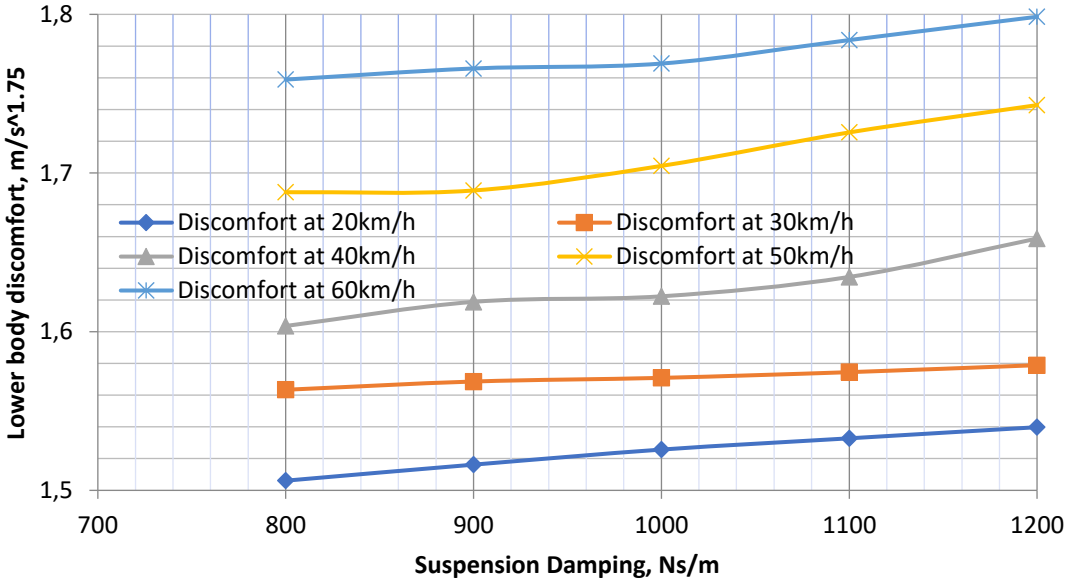

Figure 22: Discomfort at Lower body vs Suspension Damping (sprung mass, unsprung mass, suspension stiffness, tire damping and tire stiffness were constant)

Figures 23 and 24 show the effects of varying both the suspension stiffness and suspension damping on suspension travel. While there is a steady increase in suspension travel with increase in suspension stiffness, there is a gradual decrease in suspension travel with increase in suspension damping. Again, this might probably be attributed to role played by damper as shock absorber when a vehicle traversed road obstacle. Also, there was decrease in suspension travel with increase in tire stiffness. These results agreed with Olatubosun and Dunn (1991).

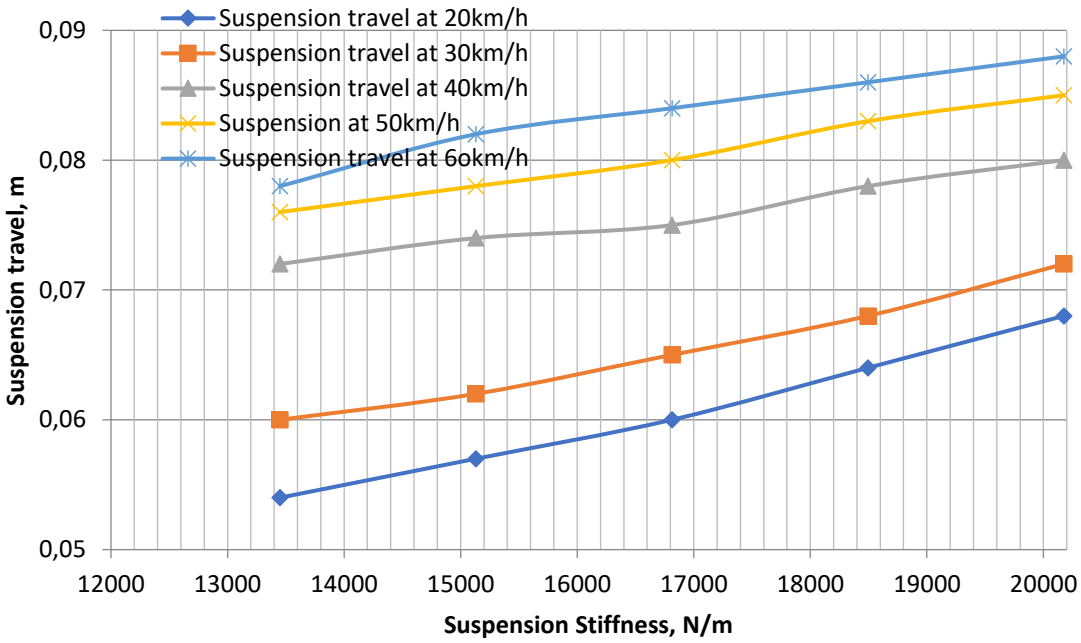

Figure 23: Variation of Suspension travel with suspension stiffness

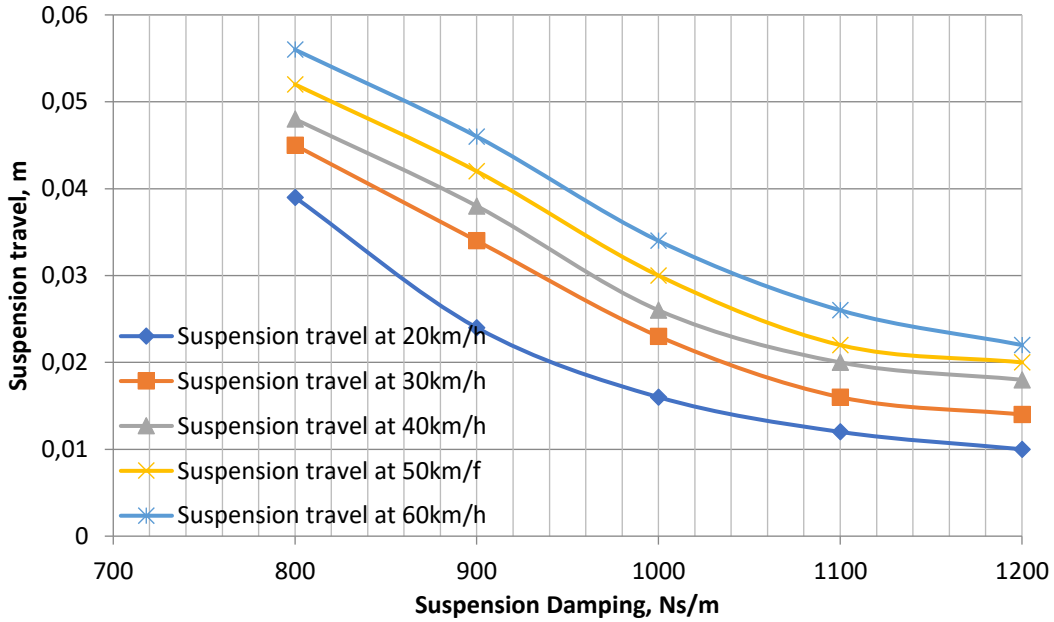

Figure 24: Variation of Suspension travel with suspension damping

Figure 25 shows the relationships between suspension travel and tire stiffness which reflects the same result as Figure 24. The variation showed a gradual decrease in suspension working space as the tire stiffness is increased. These results agreed with Olatunbosun and Dunn (1991).

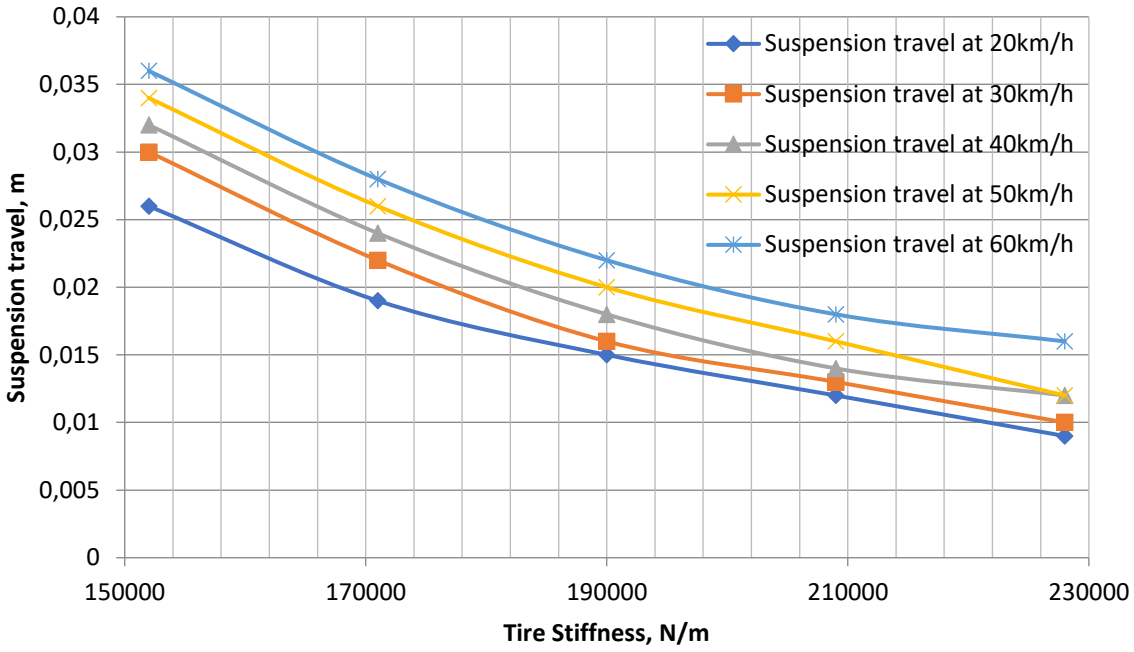

Figure 25: Variation of Suspension working Space (travel) with Tire stiffness

4. Conclusions

In this work, parametric study of rider's discomfort on passengers' vehicle with semi-active suspension system under transient road conditions was carried out. Some selected vehicle and biomechanical parameters of the human system were used to investigate the responses of the vehicle which is assumed to have traversed a half-sine obstacle with dimension 0.05 m maximum height and 0.5 m length. A Simulink block diagram based on the equations of motion of the vehicle was developed to carry out transient responses. The discomfort experienced by the driver/passenger was analyzed on the basis of vibration dose value, VDV, by varying the vehicle parameters such as sprung and unsprung masses, suspension stiffness, tire stiffness, tire and suspension dampings. The study revealed that, discomforts at the upper and lower parts of the rider's body decrease with increase in sprung mass and increase in tire damping but increase with increase in vehicle speed. It was also observed that discomforts at the upper and lower parts of the rider's body increase with increase in unsprung mass, suspension stiffness, tire stiffness, suspension damping and vehicle speeds. It is therefore concluded that unsprung mass, suspension stiffness, tire stiffness and suspension damping of a vehicle need to be improved upon (must be in good condition) at all times in order to minimize the discomfort experienced by rider on a vehicle with semi-active suspension system traversing transient road conditions.

References

Abbas. W., Abouelatta, O.B., El-Azab. M, Elsaidy. M, and Megahed. A. A., (2010). Optimization of biodynamic seated human model using generic algorithm. *SCRIP Journal of Engineering*, 2, 710-719

Akcay, H, and Turkay, S. (2009). Influence of tire on mixed H2/H synthesis of half car active suspensions, *Journal of Sound and Vibration*, 322, 15 – 28.

Alireza M., Salim H., (2006). Analysis and Design of Vehicle Suspension System Using MATLAB and SIMULINK. 2006 ASEE Annual Conference and Exposition, Chicago, Illinois. 11.213.1 - 11.213.26. DOI: 10.18260/1-2--544

Anderson, R.J; Fan, Y; (1990). *Dynamic testing and modeling of a bus shock absorber*, SAE Paper 902282.

Basso, R; (1998). Experimental characterization of damping force in shock absorber with constant velocity excitation, *Vehicle System Dynamics*, 30, 431 – 441.

Blundel, M.V., (1991). The modeling and simulation of vehicle handling Part 1: analysis method, IMechE part K, *Journal of Multibody System Dynamics*. 213, 103 – 118.

British Standard Institution BS 6841 (1987). Measurement and evaluation of human exposure to whole-body mechanical vibration and repeated shock.

Bruulsema, I.T. and McPhee, J.J., (2002). Dynamic modeling and design optimization of automobile suspension systems. *Proceeding of the CEME FORUM*, Kingston, Canada

Chace, M.A., (1967). Analysis of time-dependence of multi-freedom mechanical systems in relative coordinates. *Journal of Engineering Industry*, 89, 119 – 125.

Dixon, J.C, (2007). *The shock absorber handbook*, SAE Inc, Warrendale, PA

Duym, S; Stiens, R and Rebrouck, K; (1997). Evaluation of shock absorber model, *Vehicle System Dynamics*, 27, 109 – 127.

Faheem, A, Alam, F., (2006). The suspension dynamics analysis for a quarter car model and half car model. 3rd BSME-ASME International Conference on Thermal Engineering, Dhaka.

Fischer, D; Isermann, R. (2004). Mechatronic semi-active and active vehicle suspension. *Control Engineering Practice*. 12, 1353 – 1367.

Gohrle, C.A.; Schindler, A.; Wagner, A. and Sawodny, D., (2014) Design and vehicle implementation of preview active suspension controller, *IEEE Transactions on Control Systems Technology*, 22(3), 1135 – 1142.

Goncalves, J. P. C., Ambrosio, J. A. C. (2003). Optimization of Vehicle Suspension Systems for Improved Comfort of Road Vehicles Using Flexible Multibody Dynamics. *Nonlinear Dynamics* 34: 113–131

Griffin, M.J., (1990). *Handbook of human vibration*, Elsevier Academic Press, London.

Guglielmino, E., Sireteanu, T., Stammers, W.C., Ghita, G., Giuclea, M. (2008). Semi-active suspension control. *Improved Vehicle Ride and Road Friendliness*, London: Springer, 290-294.

Hacaambwa T. M., Giacomin, J., (2007). Subjective response to seated fore-and-aft direction whole-body vibration, *International Journal of Industrial Ergonomics*, 37, 61 – 72.

Haug, E.J., (1989). Computer aided kinematics and dynamics of mechanical system, Allyn and Bacon, Boston, USA. 1, 48 – 104.

Haug, E.J., Lin, J.S., (2002). Nonlinear active suspension design for half-car models, Proceeding of International Conference on Control and Automation, Xiamen, China, pp. 1436-1440

He, Y., McPhee, J.J., (2007). Application of optimization algorithm and multibody dynamics to ground vehicle suspension design. *International Journal of Heavy Vehicle Systems*. 14(2). 158 – 192.

Ihsan, S.I., Waleed, F., Ahmadian, M, (2007). Dynamic and control policies analysis of semi-active suspension system using a full car model, *Int. Journal of Vehicle Noise and Vibration*, 3(4), 370 – 405.

International Standard Organization (ISO) 2631, Mechanical vibration and shock evaluation of human exposure to whole body vibration- Part 1: General requirements, International Organization for Standardization, 1997

Jacquelien, M.A., Scherpen, D. J., F., Maulny, (2006). Parallel damping injection for the quarter car suspension system, Proceeding of the 17th International Symposium on mathematical theory of networks and Systems, Japan.

Jones, A.J., Saunder, D.J., (1972) Equal body contours for whole body vertical, pulse sinusoidal vibration, *Journal of Sound and Vibration*, 23, 1 – 14.

Kim, M.H.; and Choi, S.B., (2016). Estimation of road surface height for preview system using ultrasonic sensor, Proceedings of the International Conference on Networking, Sensing and Control, 1-4, IEEE.

Lin, Y., Kortum, W., (2007). Identification of system physical parameters for vehicle systems with nonlinear components, *International Journal of Vehicle Mechanics and Mobility*, 46(12), 354 – 365.

Li-Xing G., Zing, L. (2010) Vehicle vibration analysis in change speed solved by pseudoexcitation method. *Mathematical Problem in Engineering*, Hindawa Publishing Coorporation.

Li-Xing, G., Zing, L., (2010). Vehicle vibration analysis in changed speeds solved pseudoexcitation method, *Mathematical Problem in Engineering*, Hindawi Publishing Corporation

Mansfield, N.J., (2005). *Human response to vibration*, CRC Press, London.

Milliken, W.D., Milliken, W.F., (1995). *Race car dynamics*, SAE Inc, Warrendale, PA.

Niekerk, J.L; Pielemeier, W.J; Greenberg, J.A., (2002) The use of seat effective amplitude transmissibility (SEAT) values to predict dynamic seat comfort, *Journal of Sound and Vibration*, 260, 867 – 888.

Olatunbosun, O.A., Dunn, J.W., (1991). A simulation model for passive suspension ride performance optimization. Automotive Simulation' 91 (M. Heller) Springer Verlag. pp131-142.

Paddan, G.S and Griffin, M.J., (2002). Effects of seating on exposures to whole-body vibration in vehicles, *Journal of Sound and Vibration*, 253(1), pp215-241

Raji, A, Venkatachalam., (2013) Frequency response of semi-independent automobile suspension system, *International of Engineering Research and Technology*, 2(10), 654 – 661.

Ram Mohan, T., Venkata, G., Sreenivasa, K., Purushottam, A. (2010). Analysis of passive and semi-active controlled suspension systems for ride comfort in an omnibus passing over a speed bump. *International Journal of Research and Reviews in Applied Sciences*, 5(1), 7 – 17.

Rouillard, V., Sek, M.A., Bruscella, B, (2008) Simulation of road surface profiles, *Journal of Transportation Engineering*, 127, 247 – 253.

Segla, S., Reich, S; (2001). Optimization and comparison of passive, active and semi-active vehicle suspension systems, 12th IFToMN World Congrss, Besancon, France, pp1-6.

Senthil kumar, M., Vijayarangan, S; (2007). Analytical and experimental studies on active suspension system of light passenger vehicle to improve ride comfort, Technological, Mechanika 65(3), 34 – 41.

Shahriar, A., Rahman, K.A and Tanvir, S., (2016). Simulation and analysis of half-car passive suspension system. *Mechanical Engineering Research Journal*, 10, 66 – 70.

Sharp, R.S and Hassan, S.A., (1986) An evaluation of passive automotive suspension systems with variable stiffness and damping parameters, *Vehicle System Dynamics*, 15, 335 – 350.

Shirahatt, A., Prasad, P.S.S., (2008). Pravin Panzade, and Kulkarni, M.M., Optimal design of passenger car suspension for ride and road holding, *Journal of Brazil Society of Mechanical*, Science and Engineering, 30(1), 66 – 74.

Simms, A and Crolla, D., (2007). The influence of damper properties on vehicle dynamic behavior, SAE paper, 2002-01-0319.

Simon, D.E., Ahmadian, M; (2001). Vehicle evaluation of the performance of magneto-rheological dampers for heavy truck suspension, *Journal of Vibration and Acoustics*, 123(3), 365 – 375.

Soliman, A.M.A., Kaldas, M.M.S., and Abdullah, S.A., (2013). Influence of road roughness on the ride comfort and rolling resistance for passenger car, SAE, 010993.

Stutz, L. T., Rochinha, F. A., (2011). Synthesis of a Magneto-Rheological vehicle suspension system built on the variable structure control approach J. Braz. Soc. Mech. Sci. & Eng. 33(4). https://doi.org/10.1590/S1678-58782011000400008

Sun, L; (2002). Simulating pavement surface roughness and IRI based on power spectral density, *Mathematics and Computers in Simulation*, 61(2), 77 – 89.

Thite, A.N., Banvidi, S., Ibicek, T., and Bennett, L., (2011). Suspension parameter estimation in the frequency domain using a matrix inversion approach, *International Journal of Vehicle Mechanics and Mobility*, 49(12), 1803 – 1822.

Thompson, A.G., (1989). Optimum damping in a randomly excited non-linear suspension, Proceedings Institute of Mechanical Engineers, 184(2A, No. 8), 169 – 184.

Verros, G; Natsivas, S and Stepan, G; (2000) Control and dynamics of quarter car model with dual-rate damping, *Journal of Vibration and Control*, 6, 1045 – 1063.

Volker Dorsch., (2014) Simulation of vehicle dynamics control by active steering systems, *University of Applied Science*.

Wei, W., Lin, L., (2007). Vibration Control of Vehicle-bridge Dynamic Interactive System. 2007 Chinese Control Conference, Zhangjiajie, China. 21-25, doi: 10.1109/CHICC.2006.4346946.

Zhang, Z., Norbert, C., Cheung, K. W.E. Cheng, (2010) Application of Linear Switched Reluctance Motor for Active Suspension System in Electric Vehicle, *World Electric Vehicle Journal*, 4(1) 14 – 21.

Zhaoling, M; (2002). Dynamic simulation of vehicle suspension system, *Mechanical*, 29, 11 – 13.